Accepted Article

DR CHARLOTTE GROSSIORD (Orcid ID : 0000-0002-9113-3671)
DR THOMAS N BUCKLEY (Orcid ID : 0000-0001-7610-7136)
DR ROLF TW SIEGWOLF (Orcid ID : 0000-0002-0249-0651)

Article type : Commissioned Material - Tansley Review

Tansley review

Plant responses to rising vapor pressure deficit

Charlotte Grossiord[1,2], Thomas N. Buckley[3], Lucas A. Cernusak[4], Kimberly A. Novick[5], Benjamin Poulter[6], Rolf T.W. Siegwolf[1], John S. Sperry[7], Nate G. McDowell[8]

[1]Swiss Federal Institute for Forest, Snow and Landscape Research WSL, Zürcherstrasse 111, 8903 Birmensdorf, Switzerland

[2]École Polytechnique Fédérale de Lausanne EPFL, School of Architecture, Civil and Environmental Engineering ENAC, 1015 Lausanne, Switzerland

[3]Department of Plant Sciences, University of California, Davis, Davis, CA 95616, USA [4]College of Science and Engineering, James Cook University, Cairns, Queensland, Australia [5]School of Public and Environmental Affairs, Indiana University Bloomington, Bloomington, IN, USA

[6]NASA Goddard Space Flight Center, Biospheric Sciences Lab, Greenbelt, MD 20771, USA

[7]Department of Biology, University of Utah, Salt Lake City, UT, 84112, USA

[8]Earth Systems Science Division, Pacific Northwest National Laboratory, Richland, WA 99354, USA

*Charlotte Grossiord, phone: (+41) 44 739 2069, e-mail: charlotte.grossiord@wsl.ch

This article has been accepted for publication and undergone full peer review but has not been through the copyediting, typesetting, pagination and proofreading process, which may lead to differences between this version and the Version of Record. Please cite this article as doi: 10.1111/nph.16485

This article is protected by copyright. All rights reserved

Accepted Article

Received: *31 May 2019*

Accepted: *4 February 2020*

Author ORCID information:

Charlotte Grossiord: 0000-0002-9113-3671

Thomas N. Buckley: 0000-0001-7610-7136

Lucas A. Cernusak: 0000-0002-7575-5526

Benjamin Poulter: 0000-0002-9493-8600

Rolf T.W. Siegwolf: 0000-0002-0249-0651

Contents

This article is protected by copyright. All rights reserved

Accepted Article

Summary

Recent decades have been characterized by increasing temperatures worldwide, resulting in an exponential climb in vapor pressure deficit (*VPD*). *VPD* has been identified as an increasingly important driver of plant functioning in terrestrial biomes including being a major contributor in recent drought-induced plant mortality, independently from other drivers associated with climate change. Despite this, few studies have isolated the physiological response of plant functioning to high *VPD*, thus limiting our understanding and ability to predict future impacts on terrestrial ecosystems. An abundance of evidence suggests that stomatal conductance declines under high *VPD* and transpiration increases in most species up until a given *VPD* threshold, leading to a cascade of subsequent impacts including reduced photosynthesis and growth, and higher risks of carbon starvation and hydraulic failure. Incorporation of photosynthetic and hydraulic traits in 'next-generation' land-surface models has the greatest potential for improved prediction of *VPD* responses at the plant- and global-scale, and will yield more mechanistic simulations of plant responses to a changing climate. By providing a fully integrated framework and evaluation of the impacts of high *VPD* on plant function, improvements in forecasting and long-term projections of climate impacts can be made.

Keywords: mortality, productivity, stomatal conductance, transpiration, warming

This article is protected by copyright. All rights reserved

Accepted Article

I. Introduction

The amount of water vapor that the air can hold, i.e. the saturation vapor pressure, is a curvilinear function of air temperature (Lawrence, 2005). Thus, global land surface temperature rise is increasing the saturation vapor pressure of the atmosphere. However, the actual vapor pressure has not been increasing at the same rate, such that the difference between the saturation and actual vapor pressure, hereafter the vapor pressure deficit (or *VPD*), is rising (Hatfield & Prueger, 2015; Fig. 1; see Box 1 for summary of abbreviations used in the article). An increase in *VPD*, and more specifically in leaf-to-air vapor pressure deficit (VPD_L), affects plant physiology independently of other drivers associated with climate change, e.g. elevated carbon dioxide concentrations [CO_2]. High *VPD* typically causes plants to close their stomata to minimize water loss and avoid critical water tension within the xylem (Running 1976), which occurs at the cost of reduced photosynthesis. Simultaneously, transpiration rate increases with high *VPD* up to a point after which it either remains high or starts decreasing (e.g., Franks *et al*., 1997), resulting in a further exacerbation of plant water stress. Along with its direct impact on plant physiology, high *VPD* results in increased rates of water loss from moist soils, in turn causing drying and heating of the terrestrial surfaces and contributing to more frequent and severe drought events and plant water stress (Dai, 2012). As such, *VPD* is a major determinant of global water resources and plant water relations, and could become increasingly important for vegetation dynamics over upcoming decades due to its chronic, global, temperature-driven rise.

While much of our attention has been directed towards plant responses to high temperature (e.g. Hughes 2000; Lindner *et al*., 2010; Way & Oren 2010), reduced precipitation (e.g. Bréda *et al*., 2006; Allen *et al*., 2010; Knapp *et al*., 2017) and rising atmospheric carbon dioxide concentration (e.g. Ceulemans & Mousseau 1994; Ainsworth & Long 2005), the independent physiological effects of high *VPD* on vegetation dynamics remain less explored. Part of the uncertainty associated with *VPD* impacts on plants relates to the difficulty to disentangle *VPD* effects from temperature, radiation and other climate drivers of plant function (but see Novick *et al*., 2016). For instance, on a diurnal or seasonal basis, high *VPD* conditions tend to co-occur with high radiation, making it difficult to untangle their relative effects. Similarly, high *VPD* conditions also usually occur in nature concurrently with stresses such as heat waves and droughts (i.e. periods of anomalously low precipitation) that are often thought to have the dominant impact on plant physiology. However, the relative role of *VPD vs*. other climatic drivers, particularly other

This article is protected by copyright. All rights reserved

stressors associated with recent climate change, may be much higher than previously thought. For instance, extended periods of high *VPD* have been acknowledged as a primary driver of large-scale tree mortality in forest ecosystems (e.g. Breshears *et al*., 2013; Williams *et al*., 2013), as being positively correlated with wildfires (Seager *et al*., 2015; Williams *et al*., 2014), and as being responsible for reductions in crop production (e.g. Challinor & Wheeler 2008; Lobell *et al.,* 2011*;* 2013; Asseng *et al*., 2015; Zhao *et al*., 2017).

The objectives in this review are to shed light on plant responses to high *VPD*. In the different sections we (1) provide a review of fundamental knowledge on what *VPD* represents from a plant's perspective and how *VPD* is expected to shift under future climate conditions, (2) describe the mechanisms by which stomata detect and respond to variation in *VPD*, (3) highlight the variability in plant stomatal sensitivity to *VPD* across species and biomes and its potential drivers, (4) describe the recent trends in plant performance (i.e. photosynthesis, transpiration, growth and mortality) resulting from high *VPD*, and (5) discuss how plant responses to *VPD* have been and may be incorporated in the next generation of small- and large-scale dynamic vegetation models. This review addresses *VPD* impacts in all climatic regions. Most empirical studies investigating *VPD* impacts include other co-varying factors, thus impacts of *VPD* on vegetation cannot always be discussed independently of other parameters such as radiation, temperature and rising atmospheric CO_2 concentrations. Although in this review we also included studies where co-variation with other factors is present, we highlight and discuss which evidence includes other factors that could influence plant responses.

II. Rising *VPD* under global warming

Over the past 30 years, global surface temperature has risen by approx. 0.2°C per decade (IPCC, 2019). Warming increases the amount of water vapor the air can hold at saturation, i.e. the saturation water vapor pressure (e_s) (Bohren *et al*., 2000). The actual vapor pressure of the air (e_a) is constrained at the upper end by e_s so that as air temperature increase, so does the maximum amount of water vapor (equilibrium between evaporation and saturation). e_a is also dependent on the amount of moisture in the air. *VPD*, which is a direct measure of the atmospheric desiccation strength, represents the difference between e_s and e_a ($VPD = e_s\text{-}e_a = e_s - (RH \times e_s /100)$ where RH is the relative humidity in the air in percent; Monteith & Unsworth 1990). Because e_s is driven

This article is protected by copyright. All rights reserved

only by temperature, it increases during periods of high air temperature (i.e. heat waves), and results in higher *VPD* following a nonlinear relationship (De Boeck et al., 2010; Fig. 2). Long-term changes in *VPD* are still uncertain as they will depend both on e_s and on the extent of water movement limitation from the land surface to the atmosphere under future climate. While numerous studies have reported globally a constant RH under future scenarios (e.g. Dai, 2006; McCarty *et al*., 2009), others have suggested a negative (e.g. Byrne & O'Gorman, 2018) or positive (e.g. Shenbin *et al*., 2006) trend at regional scales. Nevertheless, some studies have highlighted a sharp increase in global *VPD* in recent decades (Zhang *et al*., 2015; Yuan *et al*., 2019; Fig. 1), and others have predicted a continuous rise in *VPD* over the next century using general circulation models (Williams *et al*., 2013; Ficklin & Novick 2017).

Plant scientists interested in the physiological impacts of *VPD* variation (i.e., at the leaf- or plant-level) often use VPD_L to estimate *VPD* from a plant perspective because the leaf temperature can deviate from the ambient air (higher or lower via transpirative cooling). The temperature of plant canopies is a function of energy exchange processes dependent on the amount of energy that enters via solar radiation and ambient heat, and energy that exists the canopy via heat loss, reflected light and transpired water (Monteith & Unsworth, 1990). Boundary layers surrounding each leaf or the entire canopy allow transpired water to humidify the air surrounding the leaves, uncoupling *VPD* at the leaf surface from that in the bulk air (Jarvis & McNaughton, 1986). As canopy-atmosphere coupling decreases and boundary layer increases, the role of radiation on leaf temperature becomes more important, while the role of *T* is progressively reduced. Consequently, VPD_L is the more accurate value for the evaluation of the leaf water balance (and possibly for the whole plant- and even canopy-level). VPD_L is calculated as the difference in the water vapor pressure in the leaf (usually assuming saturation vapor pressure within the stomatal pore, i.e. 100% RH, but see later sections on this assumption) minus the water vapor pressure of the ambient air (e.g., Dai *et al*., 1992; Day 2000; Marchin *et al*., 2016).

III. Mechanisms of stomatal responses to *VPD*

A rapid increase in VPD_L typically induces a decrease in steady-state stomatal aperture and stomatal conductance, g_s (Fig 3a). In seed plants (though not in seedless plants), this response is preceded by a transient change in g_s in the opposite direction; i.e., stomata "pop open" before closing following exposure to increased VPD_L (Fig 3b), within two to 25 minutes (Buckley *et al*.,

This article is protected by copyright. All rights reserved

2011). The transient response arises from a decrease in the "backpressure" imposed on stomata by epidermal cells, and the steady state response arises from an even larger drop in guard cell turgor, driven by actively-mediated efflux of osmotic solutes (Buckley 2005). Overall, no consensus exists about the exact sensing mechanisms and processes driving the stomatal closure response to increased VPD_L. In angiosperms this response is thought to involve active sensing of water status in cells somewhere within the leaf, possibly in the mesophyll, the vasculature, and/or in stomatal guard cells themselves, likely mediated by hormonal signals like abscisic acid (Saliendra *et al*., 1995; Comstock & Mencuccini 1998; Buckley 2005; McAdam & Brodribb 2016). Leaf water potential (Ψ_L) and hydraulic conductance (K_{leaf}) determine how epidermal water potential and guard cell turgor respond to changes in VPD_L (Sharpe *et al*., 1987), and thus are likely major controls of stomatal response to VPD_L (Franks & Farquhar 1999). Midday depression in g_s is common in many plant species (e.g. Schulze *et al*., 1974; Grassi *et al*., 2009), and has been associated with variation in midday stem water status (Zhang *et al*., 2013), supporting that stomatal response to VPD_L is strongly related to the leaf- but also the whole-plant hydraulic characteristics (Brodribb & Jordan 2008).

Stomatal regulation is directly responsible for controlling leaf-level transpiration (T) response to VPD_L so that when VPD_L is low and stomata are fully open, T increases linearly with VPD_L. However, the effects of VPD_L on water loss vary widely among species. By re-evaluating a large set of g_s and T responses to VPD_L, Monteith (1995) concluded that in most studies, stomatal closure was induced by guard cells sensing the increased rate of T through the stomatal pore. This "feed-back" response results in T increasing nearly in proportion to VPD_L (regime A in Monteith, 1995). However, other studies reported declining rates of T under high VPD_L (e.g. Schulze *et al*., 1972; Franks *et al*., 1997; Cunningham, 2004; Whitley *et al*., 2013). This phenomenon is known as the "feed-forward" response (Farquhar 1978). While various mechanisms have been proposed to explain this response, more experiments are still needed to improve our understanding of this topic.

Similarly, stomatal responses to diurnal variation in VPD_L can also strongly influence photosynthetic CO_2 assimilation (A) to a varying degree across species. For instance, A declined by 9.4%, 13.6%, 21,0%, 29.4% and 36.6% in Z. mays, S. townsendii, C. austral, N. tabacum, and R. communis (Long & Woolhouse, 1978; Dai *et al*., 1992; Cunningham, 2005) (see Supporting Information Fig. S1). While, to our knowledge, no study investigated impacts of high VPD_L on photosynthetic capacity (i.e. maximum carboxylation velocity V_{cmax}, and maximum rate of

This article is protected by copyright. All rights reserved

electron transport J_{max}) independently from drought or temperature impacts, some findings suggest that extended stomatal closure induced by high VPD_L could alter V_{cmax} and J_{max}. For instance, Flexas *et al*., (2006) found that stomatal closure triggers the down regulation of Rubisco activity (potentially because of decreased activation state of the enzyme) in response to a certain threshold of g_s in C_3 plants, resulting in lower V_{cmax} and J_{max}. However, the relative impact of VPD_L on V_{cmax} and J_{max}, and the physiological meaning of these hypothetical changes remains unknown, and should deserve more attention in future studies.

A critical assumption in calculations of gas exchange parameters such as g_s is that intercellular air spaces inside leaves remain saturated with water vapor, particularly when VPD_L increases to values above ca. 2 kPa (Cernusak *et al.*, 2018). To calculate g_s and intercellular CO_2 concentration (c_i), it is typically assumed that intercellular water vapor (e_i) is at saturation, so that the vapor pressure can be inferred from measurements of leaf temperature (Gaastra, 1959). Over the last 50 or so years, several attempts have been made to verify this assumption, with some results supporting it (Farquhar & Raschke, 1978; Jones & Higgs, 1980), and others suggesting that unsaturation takes place at moderate to high VPD_L (Jarvis & Slatyer, 1970; Ward & Bunce, 1986; Canny & Huang, 2006; Cernusak *et al.*, 2018). This diversity of potential unsaturation across species may reflect the dynamic nature of g_s. In species with a relatively sensitive stomatal response to VPD_L, adjustment of g_s will likely regulate T such that no appreciable unsaturation occurs (Buckley *et al.*, 2017; Cernusak *et al.*, 2019). In other species, a slower or less sensitive stomatal response may allow for unsaturation transiently or at intermediate VPD_L before stomata have closed and slowed T sufficiently (Holloway-Phillips *et al.*, 2019). Still other species may show appreciable unsaturation during steady state gas exchange at high VPD_L, as was recently observed in two semi-arid conifer species, which showed unsaturation as low as $0.8 \times e_s$, (Cernusak *et al.*, 2018). Such low values of intercellular relative humidity are challenging for our current understanding of intra-leaf water relations (Buckley & Sack, 2019), but also present an opportunity for new explorations of internal hydraulic design.

In this review, we focus on physiological responses to VPD_L at a range of scales, with the response of g_s being critical among these. One typically infers a response of g_s by measuring T and assuming saturation of e_i, so that g_s can be calculated. If e_i becomes less than saturated as VPD_L increases, then g_s will have been underestimated in those instances. However, the response of T itself will still have been measured without bias, and the response of T to VPD_L could still be

This article is protected by copyright. All rights reserved

faithfully reconstructed from the inferred g_s. The difference if e_i became unsaturated would be that the increasing resistance to T with increasing VPD_L would have actually been shared between the stomata and the mesophyll. This situation is analogous to inferring a parameter such as V_{cmax} from the response of photosynthesis to variation in c_i, but assuming that c_i is equal to c_c, the chloroplastic CO_2 concentration. This is common practice (Wullschleger, 1993; Walker *et al.*, 2014), even though it is well known that c_c is less than c_i due to mesophyll resistance to CO_2 diffusion. In the case of mesophyll resistance to transpiration, we know much less about when and to what extent it occurs. Therefore, we recommend that practitioners continue to interpret T responses to VPD_L as resulting entirely from the action of g_s, while the challenging work of better understanding the nature of unsaturation of e_i continues in parallel.

In terms of modeling the response of g_s to VPD_L, it is important to realize that most empirical datasets used to fit parameters for different vegetation types (e.g., Lin *et al.*, 2015) will have been collected under the assumption that e_i was saturated. In such a case, the impact of unsaturation, if it occurred, on T will already have been incorporated into the fitted parameters that define the stomatal response function to VPD_L. As described above, if unsaturation occurred it would have made the g_s response appear to be more sensitive to increasing VPD_L than it actually was; that is, stomata would have appeared to close more in response to increasing VPD_L than would be estimated from the physical change in aperture. Where the aim of modeling is to estimate the transpiration flux from the land surface, and if fitted parameters for modeling g_s (Franks *et al*., 2018) were defined with empirical g_s measurements that assumed e_i saturated, one should not further correct for unsaturation of e_i in modeling T. This would effectively be doubly accounting for unsaturation of e_i.

IV. Variability in sensitivity to *VPD* across species and ecosystems

1. Variability in g_s sensitivity across species

Stomatal sensitivity to VPD_L, often described in terms of the slope between g_s and $\ln(VPD_L)$ (Oren *et al*., 1999; Fig. 3a), reflects the magnitude of stomatal closure with increasing VPD_L, and therefore represents the primary strategy by which plants regulate gas exchange in response to rising VPD_L. Decades of research on stomatal behavior have highlighted that stomatal sensitivity to VPD_L is highly variable across- and within-species (e.g., Körner et al., 1979;

This article is protected by copyright. All rights reserved

Whitehead *et al*., 1981; McNaughton & Jarvis 1991; Cunningham, 2004; 2005; Creese *et al*., 2014; Gao *et al*., 2015). Even within a plant, stomatal sensitivity to VPD_L can differ between leaves that have different functions, morphology, and anatomical traits such as stomatal pore depth and density (Warrit *et al*., 1980; Appleby & Davies 1983; Streck 2002). Using empirical data, Oren *et al*., (1999) found a consistent relationship between g_s at low VPD_L (g_{sref} corresponding to g_s at 1 kPa VPD_L) and sensitivity to VPD_L, whereby plants with higher g_{sref} tend to be more sensitive to increasing VPD_L (i.e., more rapid stomatal closure). Oren *et al*., (1999) generalize this result by observing that, when the dependence of conductance on VPD is expressed as $g_s = g_{s,ref}[1-m\ln(VPD/VPD_{ref})]$, the parameter m is approx. $0.6 \times g_{sref}$ for a large range of mesic species, suggesting that stomatal regulation occurs systematically near a constant Ψ_L value. However, a reduced sensitivity was found for desert species ($m = 0.4 \times g_{sref}$), highlighting a less strict regulation of Ψ_L as VPD_L increases in more drought-tolerant species (Oren *et al*., 1999), and suggesting different sensitivities to VPD_L between plant functional groups.

These findings are consistent with the observation that leaf and stem hydraulic capacity is strongly related to stomatal sensitivity to VPD_L (Brodribb & Jordan 2008; Zhang *et al*., 2013), and attest for the fundamental role of plant hydraulics in driving stomatal aperture in response to VPD_L variation. A clear distinction in stomatal sensitivity to VPD_L could therefore be expected between isohydric and anisohydric plant species (e.g. those that hold Ψ_L more constant via stomatal closure *vs*. those that allow Ψ_L to drop more significantly; Tardieu & Simmoneau 1993), whereby the relatively isohydric species could have stronger stomatal sensitivity to VPD_L compared to anisohydric ones. For instance, Cunningham (2004) found higher stomatal sensitivity in tropical trees relative to temperate ones, and suggested that these responses could be linked to their isohydricity (i.e., higher stomatal sensitivity in isohydric species relative to anisohydric ones). However, no measure of water potential was conducted in this study to confirm this hypothesis. Although identifying such behaviors could have strong implications for vegetation models, most studies investigating isohydric/anisohydric strategies have been strongly focused on soil moisture responses (e.g. Martinez-Vilalta *et al*., 2014), and the evolution of leaf-level variables over timescales of weeks. Frameworks that mathematically link isohydricity and sensitivity to VPD_L have been recently developed (Sperry *et al*., 2017; Novick *et al*., 2019), but await extensive empirical validation, and must contend with the fact that VPD_L and soil moisture are coupled at long (weekly), but not short (i.e. diurnal) timescales. Improving our interpretation and predictive

This article is protected by copyright. All rights reserved

power will require future work to investigate how these processes vary between plant functional groups, and how trait coordination within plants relates to stomatal sensitivity to VPD_L and could vary in predictable ways along environmental gradients. Furthermore, scaling-up these leaf- or plant-level responses to VPD_L at ecosystem- or landscape-scales would be needed to assess the impacts of these different stomatal behaviors on the global water cycle and feedbacks to climate regulation.

2. Variability in G_{surf} sensitivity across ecosystems

For decades, sap flow measurements and eddy covariance flux towers have provided rich information about the relationship between canopy stomatal function and *VPD* (e.g., Pataki *et al*., 1998a; Baldocchi 2003) though caution is required when using this approach to estimate the stomatal sensitivity to *VPD* as differences between canopy and air temperature need to be accurately accounted for (Schymanski & Or 2017). Further, when using flux tower data to draw inference about transpiration and canopy conductance, care should be taken to exclude data collected when soil and canopy interception and evaporation represent a large fraction of measured evapotranspiration (*ET*) (for example, by filtering for conditions when the canopy and soil are wet, Fig. 4).

Tower-derived observations of *ET*, and also sensible heat and momentum fluxes, are sufficient to invert the Penman-Monteith (P-M) equation for *ET* to produce stand-level surface canopy conductance (G_{surf}, Kim & Verma 1991). The P-M equation (Penman 1948, Monteith 1965) is a widely used model for transpiration and *ET* that is most commonly applied at the ecosystem scale, which matches the scale at which flux tower data are collected. It blends approaches for modeling transpiration and *ET* emerging from both conservation of mass and energy. It is forced by net radiation, *VPD*, wind speed, and temperature. The model requires an estimate of both surface and aerodynamic conductance to water vapor, but the latter can be estimated with reasonable confidence from wind observations and *a priori* assumptions about key meteorological length scales (including the momentum roughness length and the zero-plane displacement, see Novick *et al*., 2016 for example). Thus, all of the input variables to the P-M equation are "known" from flux tower data except G_{surf}, so that the equation can be solved for G_{surf} to create a half-hourly timeseries. While G_{surf} is not a perfect proxy for g_s, as it contains

This article is protected by copyright. All rights reserved

information reflecting both stomatal and soil resistance to evaporation, these interactions can be minimized through careful data screening or *ET* partitioning (Sulman *et al*., 2016; Li *et al*., 2019).

Across sites and biomes, G_{surf} measurements consistently confirm the typical inverse and non-linear relationship between conductance and *VPD* (Novick *et al*., 2016; Li *et al*., 2019, Fig. 4). From one site to the next, the parameters of the relationship between tower-derived G_{surf} and *VPD* vary, reflecting cross-site differences in canopy structure, soil properties, and species. For instance, using *ET* measurements, and derived G_{surf} estimations from 38 Ameriflux sites spanning a wide range of biomes, Novick *et al*., (2016) demonstrated that the relationship between G_{surf} and *VPD* is dependent on moisture regimes. Moreover, the sensitivity of G_{surf} to *VPD* was strongly reduced when moving from mesic to xeric sites (Fig. 4), suggesting stronger *VPD* control on gas exchange in wetter regions relative to drier ones. Furthermore, these findings suggest that the relative importance of *VPD* in driving G_{surf} may be especially increased in mesic ecosystems in the future with global warming (Novick *et al*., 2016), as $dG_{surf}/dVPD$ is especially steep when *VPD* is relatively low, consistent with hydraulic theory (McDowell &Allen 2015). At the same time, stomatal sensitivity to *VPD* can also shift within a given ecosystem in response to climatic variability. For example, atmospheric warming and increased *VPD* were found to reduce stomatal sensitivity to *VPD*, resulting in deterioration of water dynamics and reduced gas exchange, independently of precipitation regimes (Grossiord *et al*., 2018). Interestingly, this response varied between isohydric and anisohydric species, suggesting some link between isohydricity and sensitivity to *VPD* (Grossiord *et al*., 2017b).

However, when structural, functional and climatic characteristics of the biome are controlled for by dividing the G_{surf} by a reference conductance at *VPD* = 1 kPa, the relationship between G_{surf} and *VPD* becomes much more generic across sites (Novick *et al*., 2016; Li *et al*., 2018, Fig. 4). Specifically, the ecosystem-scale *m* is 0.5 ± -0.07 when ensemble-averaged across sites. This result agrees well with theory, and species leaf-level results, as described in the last section (e.g. Oren *et al*., 1999), and confirming the usefulness of G_{surf} as a proxy for stomatal conductance. Encouragingly, analysis of G_{surf} estimated from weather station data using the so-called ETRHEQ approach (for Evapotranspiration from Relative Humidity at Equilibrium) also produced reasonable convergence in the normalized *VPD* response across sites (Rigden *et al*., 2018). While not a direct observation of *ET*, the ETRHEQ is highly data-driven, and shows great potential for increasing our understanding of *ET* and G_{surf} dynamics in biomes where

This article is protected by copyright. All rights reserved

meteorological stations are more abundant than flux towers. Ultimately, these ecosystem-scale relationships have many practical uses and applications. Most land-surface models have a stand-scale resolution, and new approaches representing stomatal sensitivity to *VPD* benefit from testing with ecosystem-scale data (e.g. Bonan *et al*., 2014; Franks *et al*., 2018). They could also inject dynamic plant feedbacks into drought monitoring indices like the Palmer Drought Severity Index, particularly if those indices use a P-M type formulation to represent *ET* (Ficklin *et al*., 2015). Finally, estimates of conductance from flux towers already have a rich and continuing history of being blended with remotely-sensed vegetation indices and models like P-M to develop coarse-scale conductance and *ET* data products (Hulley *et al*., 2017).

V. Impact of high *VPD* on carbon and water relations and drought-induced mortality

1. Transpiration, photosynthesis and gross ecosystem productivity responses to high VPD

Plant- and ecosystem-level transpiration responses to increasing *VPD* are complex, and encompass increasing and decreasing water use and sap flux velocity depending on the range of *VPD* and on other environmental variables like soil moisture (Whitehead & Jarvis 1981; Benyon *et al*., 2001). Earlier work has shown that although leaf water potentials and g_s strongly decrease with rising *VPD*, transpiration rates tend to increase and remain high for a wide range of species originating from distinct habitats, consistent with the "feed-back" response discussed in section III (Granier *et al*., 1992; Pataki *et al*., 1998b; O'Grady *et al*., 1999; Meinzer *et al*., 2003; Bovard *et al*., 2005; Hölscher *et al*., 2005; Kupper *et al*., 2011, but see Whitley *et al*., 2013 among others for evidence of a "feed-forward" response leading to reduced *T* with high *VPD*). This response leads to a more rapid depletion of soil moisture, thereby increasing the risk of experiencing drought stress faster, particularly if high *VPD* conditions are combined with reduced precipitation (Will *et al*., 2013; Duan *et al*., 2014).

Photosynthetic carbon assimilation (A) is directly related to stomatal conductance, but this relationship is mediated by the intrinsic water use efficiency (iWUE = A/g_s), so that the response of photosynthesis to *VPD* depends on the stomatal sensitivity to *VPD*, but also on the extent to which iWUE itself changes as *VPD* rises. Some clues about the nature of the iWUE=f(*VPD*) relationship emerge from gas exchange theory, which implies a saturating (or hyperbolic) relationship between A and g_s (Farquhar & Sharkey, 1982). When *VPD* is relatively low, initial

This article is protected by copyright. All rights reserved

increases in *VPD* will reduce g_s but not *A*, such that iWUE increases with increasing *VPD*. However, eventually, severe restrictions to g_s imposed by high *VPD* will limit *A*, which may be independently decreased by declining soil moisture and non-stomatal limitations to biochemical capacity, including reduced mesophyll conductance (Flexas et al. 2012). As a result, iWUE will saturate or even decline as *VPD* continues to rise. Thus, the overall relationship between iWUE and *VPD* is likely hyperbolic (Zhang *et al*., 2019), and the sensitivity of photosynthesis to *VPD* will likely be weaker than the sensitivity of conductance to *VPD*.

Both tree-rings and eddy covariance flux towers are useful tools for testing this prediction across sites and over long periods of time. The isotopic composition of tree rings can be analyzed for information about historic change in iWUE (Francey & Farquhar 1982). Flux towers provide information about stand level photosynthesis (i.e. gross ecosystem productivity, or *GEP*) as well as surface conductance, such that stand-level iWUE can be calculated as GEP/G_{surf}. Several recent studies have focused explicitly on the sensitivity of iWUE and *GEP* to historic changes in *VPD*. Although these studies commonly do not separate temperature from *VPD* impacts, the effects of rising CO_2 were accounted for by using various statistical approaches such as removing low-frequency trends (e.g. Andreu-Hayles *et al*., 2011) or partial least squares regressions (e.g. Wang *et al*., 2018). In general, these studies find that the relationship between iWUE and *VPD* is positive (Andreu-Hayles *et al*., 2011; Franks *et al*., 2015; Wang *et al*., 2018), with the predicted unimodal relationship between iWUE and *VPD* being observed in some sites that experience exceptionally high *VPD*. Practically, and as illustrated in Fig. 4, this means that the sensitivity of photosynthesis to *VPD* is relatively less than the sensitivity of conductance to *VPD*, but nonetheless substantial. Moreover, several recent tree-ring studies identify rising *VPD* (considered concurrently with increasing temperature) as an important limitation to tree growth (Williams *et al*., 2013; Babst *et al*., 2019; Yi *et al*., 2019), suggesting that among other processes (e.g. reduction in phloem transport), reductions to photosynthesis at high *VPD* could be sufficient to limit the supply of carbon to growth sinks, at least for current climate conditions.

Moreover, to persist in response to high temperature and *VPD* rise, plants will need to regulate their temperature, particularly of photosynthetically-active tissues. During periods of optimum soil water supply and non-limiting VPD_L, plants can passively thermoregulate their foliar temperature with their transpiration flux (Mahan & Upchurch 1988). The "cooling effect" of *T* arises because a substantial amount of energy that would otherwise heat the leaf is used to convert

This article is protected by copyright. All rights reserved

each mole of liquid water to water vapor. Extended periods of high *T* (resulting from high *VPD*) could result in an impaired cooling of leaves, and in heating of plant canopies (Gates 1968), particularly if combined with drought-stress. In general, plants can adjust efficiently to higher temperatures by shifting their temperature optimum, in temperate regions within a few hours. However, when canopy temperatures are chronically beyond an optimal temperature threshold, photosynthetic rates will decrease and reduce the capacity of plants to perform vital functions, including taking up carbon from the atmosphere through photosynthesis (Berry & Bjorkman, 1980). At high foliar temperature mostly occurring during heat waves and depending on the duration of exposure (T_{leaf} >40°C), cellular injury such as protein denaturation, inactivation of enzymes in chloroplasts, loss of membrane integrity or even cell death can occur, leading to a lethal collapse of the cellular organization (Teskey *et al*., 2015; Wahid *et al*., 2007). These injuries eventually lead to inhibition of growth and diminish photosynthetic uptake of carbon. As heat waves are often, but not always, accompanied by drought the susceptibility to heat induced damages is exacerbated significantly. However, although foliar thermoregulation is a crucial process for the long-term maintenance of terrestrial ecosystems, few studies have investigated the mechanisms driving this process, the interaction between thermoregulation, plant water relations, and high *VPD*, and their feedbacks to ecosystem resilience.

2. Role of high VPD in drought-induced plant mortality

Elevated *VPD* has been implicated as having a significant role in recent and future drought-associated mortality events (Breshears *et al*., 2013; Stovall *et al*., 2019). Observations of recent vegetation die-offs (widespread and fast mortality events) of conifers in southwestern USA have been more strongly correlated with *VPD* than with either temperature or precipitation anomalies (Williams *et al*., 2013). For conifers throughout the northern hemisphere, the implication of rising *VPD* is widespread range reductions due to elevated mortality (McDowell *et al*., 2016). Rising *VPD* may also be involved in driving increased Amazonian tree mortality (Brienen *et al*., 2015; McDowell *et al*., 2018). Consistent with this, multiple studies have droughted trees to death more rapidly via elevated temperature treatments in greenhouse settings (Adams *et al*., 2009; Will *et al*., 2013; Zhao *et al*., 2013), but no manipulative mortality studies have yet attempted to disentangle the impacts of elevated *VPD* and high temperature.

This article is protected by copyright. All rights reserved

In addition to the observations of growth and mortality that are consistent with a growing *VPD* limitation, theory suggests that rising *VPD* must impact plant hydraulics such that vegetation shifts, including rapid mortality, are likely. Fundamentally, the mechanisms by which rising *VPD* may accelerate the risk of mortality are consistent with the transpiration and stomatal responses to *VPD*. Specifically, if elevated *VPD* causes elevated *ET* it should increase the risk of hydraulic failure, or catastrophic dehydration, by exacerbating the water potential drop within foliage and wood (Will *et al*., 2013; Cochard 2019). This effect is amplified by an enhanced *VPD*-driven evaporation resulting in soil water loss and desiccation, increasing drought stress via lack of soil water (Fig. 5a). Ultimately, higher *ET* should result in less time required to reach a threshold beyond which *ET* must decline and as hydraulic failure (defined as the percentage loss of conductance in Fig. 5a) must increase. Stomatal closure during periods of elevated *VPD* may also promote declining growth and allocation to carbohydrates via reduced photosynthesis (Fig. 5b), which if the stomatal closure is sufficiently strong and prolonged, could lead to carbon starvation (Martinez-Vilalta *et al*., 2002) including failure to defend against biotic attack (Fig. 5c; McDowell et *al*., 2011).

Long-term field experiments where atmospheric temperature and *VPD* are manipulated and combined are particularly useful for anticipating the impacts of rising *VPD* on plant mortality risks, particularly as the effects may occur in cascades (i.e., short *vs*. long-term impacts, Fig. 5). Several systems have been established where the independent and combined effects of drought, heat stress or high atmospheric [CO_2] are tested on tree functioning (e.g. Hanson *et al*., 2011; Grossiord *et al*., 2017a), but to our knowledge only one field experiment manipulates *VPD*, independently from other drivers (Kupper *et al*., 2011). Using mist fumigation in experimental forest plots in south-eastern Estonia, the free air humidity manipulation (FAHM) increase air humidity over ambient levels, thereby reducing *VPD*. The experiment revealed that high humidity (i.e., low *VPD*) resulted in reduced *T*, aboveground growth and photosynthesis (reviewed in Oksanen *et al*., 2018). However, while some effects may be attributed to reduced *VPD*, others may be partially explained by the condensation of water onto the leaf surface induced by the misting system employed at the site. Water retention on the leaf surface could directly impair stomatal functioning, gas exchange and photosynthesis (Ishibashi & Terashima, 1995). New experiments combining multiple stresses (e.g. *VPD* × temperature or *VPD* × drought) are urgently needed to help bring some light on the longer-term plant survival under rising *VPD*.

This article is protected by copyright. All rights reserved

Accepted Article

VI. Modeling plant and ecosystem responses to vapor pressure deficit

1. At the plant-level

Three approaches can be distinguished for modeling the stomatal response to vapor pressure deficit: mechanistic, empirical, and goal-oriented. Mechanistic models predict the stomatal response from known or hypothetical stimulus-response pathways (Buckley & Mott 2013; Pieruschka *et al*., 2010). They are useful for studying these pathways and directing their further study but the physiological parameters in some versions of such models are difficult to estimate experimentally, making them impractical for general predictive purposes (Buckley & Mott 2013). However, mechanistic models have been successfully adapted and applied in woody crops (e.g., Diaz-Espejo *et al*., 2012; Rodriguez-Dominguez *et al*., 2016) and forest trees (e.g., Buckley *et al.*, 2012; Wang *et al*., 2016).

The empirical approach to modeling the G_L response to VPD_L (as actively controlled by the stomatal g_s component) does not require mechanistic closure and is perhaps most widely used for prediction (Kennedy *et al.* 2019; Rowland *et al.* 2015). The stereotypical stomatal closure response to increasing VPD_L lends itself to curve fitting, and a host of similar equations have been used to express G_L as monotonically declining with VPD_L (Fig. 6a). Multiplying the f(VPD_L) function by the photosynthetic rate (A) can account for independent interactions with photosynthesis (as in Fig. 6a: hyperbolic, inverse, inverse sqrt, Jarvis, Ball-Berry curves) (Leuning 1995). The curve fitting parameters determine a maximum G_L at low VPD_L and determine the rate of G_L decline as VPD_L increases (the stomatal sensitivity to VPD_L). Once fitted to past data, the parameters are used to extrapolate the future. One challenge is knowing which model is best for every situation, because though qualitatively similar in representing stomatal closure with VPD_L (6A), there are fundamental differences in the transpiration response (Fig. 6b). Some functions predict a peak in T, others a plateau or gradual rise, one gives a flat T response (inverse without A), and one a decline (inverse with A). Another challenge is that the fitted parameters for the chosen model will vary within species as factors such as soil moisture or CO_2 concentration change, and they will vary across species. Progress can be made by recognizing that greater maximum G_L correlates with greater sensitivity (Kaufman 1982; Oren *et al.* 1999; Yong *et al.* 1997) and that maximum G_L is also a function of soil moisture, ambient CO_2, and other environmental cues (Leuning 1995). More curve fitting can be used to handle these interactions

This article is protected by copyright. All rights reserved

for particular situations (Jarvis 1976), but in the absence of any guiding principle the empirical approach is difficult to generalize with confidence.

Goal-oriented modeling based on an optimization criterion has the greatest potential for prediction. If we assume a physiological objective of stomatal regulation, and if we can model that objective, we automatically know how the stomata must behave in any situation to realize the assumed goal. Such a model will be equally consistent in its predictions regardless of the combination of environmental stimuli or underlying mechanism. An early goal-oriented model proposed that stomata regulate so as to maximize the cumulative photosynthesis for a fixed amount of cumulative transpiration over a given period of time (Cowan & Farquhar 1977). This predicts that stomata act to maintain $dT/dA = \lambda$, where λ is the Lagrangian multiplier for this constrained-optimization problem. The challenge is *a priori* knowledge of what λ should be as a function of plant and environment. Without knowing what λ should be ahead of time, the modeler is effectively using an empirical approach where λ is derived by fitting data (e.g. Fig. 6, blue dashed; (Medlyn *et al.* 2011).

A more tractable stomatal goal is to prevent leaf xylem pressure (P) from ever dropping below some threshold (P_t) which represents the onset of stress-induced damage such as loss of turgor or hydraulic conductance (Oren *et al.* 1999; Pieruschka *et al.* 2010; Tyree & Sperry 1988). The stomatal response at $P = P_t$ and steady-state is calculated as $G_L = K/ VPD_L \bullet (P_{soil}-P_t)$, where K is the soil-to-canopy hydraulic conductance per leaf area and P_{soil} is the soil water potential (Fig. 6, yellow dashed "inverse-A" curve). This equation incorporates plant hydraulic traits into the G_L response and predicts several observations (Oren et al. 1999): a) As P falls to P_t, G_L approaches an inverse function of increasing VPD_L, which is broadly consistent with empirical equations for the VPD response (Fig. 6a, compare yellow-dashed line), b) G_L at a given limiting VPD_L decreases with more negative P_{soil}, c) G_L sensitivity to VPD_L increases with a greater maximum G_L, d) G_L scales proportionately with K, e) The initial rise in T with VPD_L saturates as P approaches P_t. f) A decline in T that is occasionally seen at high VPD_L (Franks *et al.* 1997) is consistent with a drop in K under such conditions. Easy to implement, and consistent with at least some mechanistic hypotheses (Pieruschka *et al.* 2010), such a scheme can improve large scale models (Williams *et al.* 1996). But the approach is too simple. It predicts a strictly isohydric response to rising VPD_L (Fig. 6b, T is constant with VPD_L; yellow dashed line) and falling P_{soil}, when most species are anisohydric in allowing P to become more negative (Martinez-Vilalta *et al.* 2014). Moreover, by itself the approach cannot account for the independent feedbacks between photosynthesis and G_L.

This article is protected by copyright. All rights reserved

More recent goal-oriented approaches also incorporate plant hydraulics, but propose that stomata balance the stress-related risk of opening with the opportunity for photosynthetic gain (Mencuccini *et al.* 2019; Wolf *et al.* 2016). The risk can be calculated from a cavitation vulnerability curve, and it eventually rises non-linearly with continued stomatal opening, reaching a maximum when T induces complete hydraulic failure. The gain rises immediately on stomatal opening and continues to a maximum as modeled photosynthesis saturates. Setting the maximum risk and gain to 1 gives them equal weight in the trade-off, and the actual stomatal opening that maximizes the gain minus the risk at that instant can be calculated (Sperry *et al.* 2017). This algorithm produces a VPD_L response very similar to many empirical models (Fig. 6, red lines), and integrates interactions with light, temperature, ambient CO_2, and soil moisture. The degree of anisohydry (i.e., the degree to which T increases with VPD_L; Fig. 6b red line) is dictated by photosynthetic capacity and vulnerability to cavitation. Importantly, the responses can be predicted *a priori* from traits of photosynthetic and hydraulic capacity. Quantitatively the gain-risk approach fits experimental observations as well or better than empirical models (Venturas *et al.* 2018; Wang *et al.* 2019). Different formulations of the optimal gain *vs*. stress trade-off are possible (Eller *et al.* 2019; Mencuccini *et al.* 2019), including additional considerations such as phloem export (Hölttä *et al.* 2017; Huang *et al.* 2018). But the temptation to complicate comes at the risk of adding unknown parameters which have to be retroactively fit, reducing predicting power. Nevertheless, modeling the stomatal response from a gain *vs*. stress trade-off appears to be a promising way to improve over the purely empirical approach.

2. At the global-level

Land-surface models represent processes that regulate the exchange of carbon, water and energy fluxes between the atmosphere and biosphere by coupling plant physiology with vegetation dynamics (Sellers *et al*., 1996). Despite a large variety of land-surface modeling approaches, the models are similar in that they aim to scale processes that occur at the leaf- and individual organism-level to investigate global-scale questions and can be applied in either offline or fully coupled 'online' simulations with general circulation models providing meteorology. A range of land-surface modeling approaches exist where at the highest level, models can be split between whether they use diagnostic or prognostic approaches, with diagnostic approaches combining simple light-use efficiency models with remote-sensing observations for variables like the

This article is protected by copyright. All rights reserved

normalized difference vegetation index, leaf area index or soil moisture, for example (see Yuan *et al*., 2019). In contrast, prognostic models aim to represent ecosystem dynamics with numerical representations of processes using semi-empirical to fully mechanistic approaches (Bonan *et al*., 2003). These include the category of 'dynamic global vegetation models' that represent demography via establishment, growth and mortality (Sitch *et al*., 2013).

Plant physiological responses to *VPD* are linked to vegetation mortality in land-surface models in one or more of several interacting ways, these include; carbon deficits via negative net primary production (*NPP*) or declines in growth efficiency and water stress via hydraulic failure, in addition to mortality via non-*VPD* related processes such as heat stress or light competition (Prentice *et al*., 2007; McDowell *et al*., 2011). Land-surface models operate on the principle of balancing water demand with water supply. The models generally compute atmospheric water demand, i.e., E_{demand} or *VPD*, by using gridded fields of observed or simulated vapor pressure (Harris *et al*., 2013) using the Penman-Monteith approach and estimate the assumed saturated vapor pressure within the leaf, from air temperature or with simple biophysical models to estimate leaf temperature. Alternatively, E_{demand} can be estimated from empirical relationships relating evaporation efficiency and surface conductance with air temperature and longwave radiation (Monteith 1995). Land-surface models diverge in terms of how E_{demand} is related to g_s. Models with sub-daily timesteps, such as CLM (Bonan *et al*., 2003), ORCHIDEE (Krinner *et al*., 2005), ED (Moorcroft *et al*., 2001) or JULES (Best *et al*., 2011), use modifications of the Ball-Berry model (Ball *et al*., 1987) to relate *VPD* to g_s. Other models, with daily or greater timesteps, i.e., LPJ (Sitch *et al*., 2003), modify non-water stressed conductance by the ratio of E_{demand} and E_{supply}, where E_{supply} is related to plant available water in the soil column. In both approaches, stomatal closure induced by increasing *VPD* leads to less *GEP* and thus lower growth efficiency or negative *NPP* related mortality.

Alternative schemes for linking *VPD* with plant mortality use a hydraulic architecture approach to estimate the water-potential along a soil-plant-atmosphere continuum. This modeling approach, also known as SPA, or the soil-plant-atmosphere canopy model (Williams *et al*., 1996), calculates the transport of water, i.e., the supply, as proportional to hydraulic gradients and resistances along the continuum. Water potentials for the soil, stem and leaves, emerge as prognostic variables related to water availability, tree height, and tissue properties. The implementation of SPA-based modeling theory into land-surface models is an active area of research (Hickler *et al*., 2006; Bonan *et al.*, 2014; Christofferson *et al*., 2014; Mencuccini *et al*.,

This article is protected by copyright. All rights reserved

2019) as it provides a more mechanistic approach for linking g_s with atmospheric water demand and soil water availability. In addition, hydraulic architecture modeling approaches provide a more direct link to simulating mortality because of how they control hydraulic failure and xylem cavitation (McDowell *et al*., 2011). Modeling approaches simulate the loss of conductance due to cavitation as an s-shaped vulnerability curve, where cavitation is related to water-potential that causes a 50% loss of conductivity (Tyree and Sperry 1989; Hickler *et al*., 2006). Some land-surface models incorporate acclimation processes by altering carbon allocation to above (stem) and belowground (root) pools, which can then feedback into modifying the whole-pathway resistances that contribute to the leaf water potentials and ultimately, the leaf conductance (Hickler *et al*., 2006).

Simulated leaf and canopy conductance, their environmental responses, and interannual and decadal dynamics are evaluated using a range of techniques (Yuan *et al*., 2019). These include comparisons with flux towers (Blyth *et al*., 2010; Raczka *et al*., 2013), tree rings (Frank *et al*., 2015), and cuvette measurements (Cernusak *et al.*, 2013). Key questions on the relationship between the global carbon and water cycles have been advanced by understanding the role of *VPD* and canopy conductance processes that bridge spatial scales (Jung *et al*., 2017), soil moisture (Humphrey *et al*., 2018) and vegetation dynamics (Stocker *et al*., 2019). These studies include broader insights into hydrologic responses to *VPD* via changes in runoff, coupling with the atmosphere due to adjustments in surface roughness, and partitioning of radiation *vs*. *VPD* effects on photosynthesis (Roderick *et al*., 2014; Greve *et al*., 2017).

VII. Conclusion

Global *VPD* has increased over recent decades (Fig. 1), and is expected to continue rising in the future. High *VPD* conditions reduce stomatal conductance and photosynthesis while simultaneously increasing plant water losses through transpiration. Although these impacts vary across biomes and plant functional types, and may be mitigated in part on the long-term by increasing CO_2 concentrations, they will likely result in reduced primary productivity and amplified drought-induced plant mortality worldwide. To enable mechanistic predictions of future *VPD* impacts at local- and global-scales, key processes driving plant responses to *VPD* need to be addressed in future work. Many advances have been made in recent years in our modeling approaches of *VPD* impacts at plant- and global-scales, but future developments will require further progress in our empirical knowledge of plant responses to rising *VPD*. For instance, no

This article is protected by copyright. All rights reserved

consensus exists about the exact sensing mechanisms driving stomatal closure to rising *VPD* (and whether they respond differently to temperature- *vs*. humidity-driven changes in *VPD*), and how these mechanisms may vary between plant functional groups or along environmental gradients. Future work should focus on separating temperature *vs*. humidity driven impacts of *VPD* by using controlled experiments (e.g. growth chambers; humidity manipulation in the field), possibly across a broad range of species. Furthermore, modeling and empirical efforts should be directed towards the antagonistic impacts of *VPD* rise and other projected changes such as increasing atmospheric CO_2 concentrations, reduced precipitation and global warming.

Accepted Article

This article is protected by copyright. All rights reserved

Acknowledgements

CG was supported by the Swiss National Science Foundation SNF (5231.00639.001.01). TNB was supported by the National Science Foundation (Award 1557906) and the USDA National Institute of Food and Agriculture (NIFA) (Hatch project 1016439). BP was supported by the NASA Terrestrial Ecology Program. KN was supported by the USDA NIFA Agriculture and Food Research Initiative (Grant 2017-67013-26191) and NSF (Award 1552747). We would like to thank the reviewers and the editor for their thoughtful comments and efforts towards improving the manuscript.

Accepted Article

This article is protected by copyright. All rights reserved

Accepted Article

References

Adams HD, Guardiola-Claramonte M, Barron-Gafford GA, Villegas JC, Breshears DD, Zou CB, Troch PA, Huxman TE. 2009. Temperature sensitivity of drought-induced tree mortality portends increased regional die-off under global-change-type drought. *Proceedings of the national academy of sciences* 106: 7063-6.

Ainsworth EA & Long SP. 2005. What have we learned from 15 years of free-air CO_2 enrichment (FACE)? A meta-analytic review of the responses of photosynthesis, canopy properties and plant production to rising CO_2. *New Phytologist* **165**: 351-372.

Allen CD, Macalady AK, Chenchouni H, Bachelet D, McDowelle N, Vennetier M, Kitzberger T, Rigling A, Breshears DD, Hogg EH *et al*., 2010. A global overview of drought and heat-induced tree mortality reveals emerging climate change risks for forests. *Forest Ecology and Management* **259**: 660-684.

Anderson DB. 1936. Relative humidity or vapor pressure deficit. *Ecology* **17**: 277–282.

Andreu-Hayles L, PLanells O, Guiterrez E, Muntan E, Helle G, Anchukaitis KJ, Schleser GH. 2011. Long tree-ring chronologies reveal 20th century increases in water-use efficiency but no enhancement of tree growth at five Iberian pine forests. *Global Change Biology **17***: 2095-2112.

Appleby RF, Davies WJ. 1983. A possible evaporation site in the guard cell wall and the influence of leaf structure on the humidity response by stomata of woody plants. *Oecologi,* **56**: 30–40

Asseng S, Ewert F, Martre P, Rötter RP, Lobell DB, Cammarano D, Kimball BA, Ottman MJ, Wall GW, White JW, Reynolds MP. 2015. Rising temperatures reduce global wheat production. *Nature climate change* **5**:143.

Ball JT, Woodrow IE, Berry JA. 1987. A model predicting stomatal conductance and its contribution to the control of photosynthesis under different environmental conditions. In: Biggins J. (eds) Progress in Photosynthesis Research. Springer, Dordrecht, Netherlands.

Babst F, Bouriaud O, Poulter B, Trouet V, Girardin MP, Frank DC. 2019. Twentieth century redistribution in climatic drivers of global tree growth. *Science Advances* **5**: eaat4313.

Baldocchi DD. 2003. Assessing the eddy covariance technique for evaluating carbon dioxide exchange rates of ecosystems: past, present and future. *Global Change Biology* **9**: 479-492.

This article is protected by copyright. All rights reserved

Beer C, Ciais P, Reichstein M, Baldocchi D, Law BE, Papale D, Soussana JF, Ammann C, Buchmann N, Frank D, Gianelle D. 2009. Temporal and among-site variability of inherent water use efficiency at the ecosystem level. *Global biogeochemical cycles* 23: 2.

Berry J, Bjorkman O. 1980. Photosynthetic response and adaptation to temperature in higher plants. *Annual Review of Plant Physiology* **31**: 491-543.

Best MJ, Pryor M, Clark DB, Rooney GG, Essery R, Ménard CB, Edwards JM, Hendry MA, Porson A, Gedney N, Mercado LM. 2011. The Joint UK Land Environment Simulator (JULES), model description–Part 1: energy and water fluxes. *Geoscientific Model Development* **4**: 677-99.

Blyth E, Gash J, Lloyd A, Pryor M, Weedon GP, Shuttleworth J. 2010. Evaluating the JULES land surface model energy fluxes using FLUXNET data. *Journal of Hydrometeorology* **11**: 509-19.

Bonan GB, Levis S, Sitch S, Vertenstein M, Oleson KW. 2003. A dynamic global vegetation model for use with climate models: concepts and description of simulated vegetation dynamics. *Global Change Biology* **9**: 1543–1566.

Bonan GB, Williams M, Fisher RA, Oleson KW. 2014. Modeling stomatal conductance in the earth system: linking leaf water-use efficiency and water transport along the soil–plant–atmosphere continuum. *Geoscientific Model Development* **7**: pp.2193-2222.

Bovard BD, Curtis PS, Vogel CS, Su HB, Schmid HP. 2005. Environmental controls on sap flow in a northern hardwood forest. *Tree Physiology* **25**: 31-38.

Bréda N, Huc R, Granier A, Dreyer E. 2006. Temperate forest trees and stands under severe drought: a review of ecophysiological responses, adaptation processes and long-term consequences. *Annals of Forest Science* **63**: 625-644.

Breshears DD, Adams HD, Eamus D, McDowell NG, Law DJ, Will RE, Williams AP, Zou CB. 2013. The critical amplifying role of increasing atmospheric moisture demand on tree mortality and associated regional die-off. *Frontiers in Plant Science* **4**: 266.

Brienen RJ, Phillips OL, Feldpausch TR, Gloor E, Baker TR, Lloyd J, Lopez-Gonzalez G, Monteagudo-Mendoza A, Malhi Y, Lewis SL *et al.* 2015. Long-term decline of the Amazon carbon sink. *Nature* **519**: 344.

This article is protected by copyright. All rights reserved

Buckley TN. 2005. The control of stomata by water balance (Tansley Review). *New Phytologist* **168**: 275-292.

Buckley TN, Sack L, Gilbert ME. 2011. The role of bundle sheath extensions and life form in stomatal responses to leaf water status. *Plant Physiology* **156**: 962-973.

Buckley TN, Turnbull TL, Adams MA. 2012. Simple models for stomatal conductance derived from a process model: cross-validation against sap flux data. *Plant, cell & environment* **35**: 1647-1662.

Buckley TN, Mott KA. 2013. Modelling stomatal conductance in response to environmental factors. *Plant Cell and Environment* **36**: 1691-1699.

Buckley TN. 2016. Commentary: Stomatal responses to humidity: has the "black box" finally been opened? *Plant, Cell & Environment* **39**: 482-484

Buckley TN, John GP, Scoffoni C, Sack L. 2017. The sites of evaporation within leaves. *Plant Physiology* **173**: 1763-1782

Buckley TN & Sack L. 2019. The humidity inside leaves and why you should care: implications of unsaturation of leaf intercellular airspaces. *American Journal of Botany* **106**: 618-621.

Byrne MP & O'Gorman PA. 2013. Link between land-ocean warming contrast and surface relative humidities in simulations with coupled climate models. *Geophysical Research Letters* **40**: 5223-5227.

Byrne MP & O'Gorman PA. 2018. Trends in continental temperature and humidity directly linked to ocean warming. *Proceedings of the National Academy of Sciences* **115**: 4863-4868.

Canny MJ, Huang CX. 2006. Leaf water content and palisade cell size. *New Phytologist* **170**: 75-85.

Castellvi F, Perez PJ, Stockle CO, Ibanez M. 1997. Methods for estimating vapor pressure deficit at a regional scale depending on data availability. *Agricultural and Forest Meteorology* **87**: 243-252.

Cernusak LA, Goldsmith G, Arend M, Siegwolf RTW. 2019. Effect of vapor pressure deficit on gas exchange in wild-type and abscisic acid-insensitive plants. *Plant Physiology* **181**: 1573-1586.

This article is protected by copyright. All rights reserved

Cernusak LA, Winter K, Dalling JW, Holtum JAM, Jaramillo C, Korner C,. Leakey ADB, Norby JR, Poulter B, Turner BL, Wright SJ. 2013. Tropical forest responses to increasing atmospheric CO_2: current knowledge and opportunities for future research. *Functional Plant Biology* **40**: 531–551.

Cernusak LA, Ubierna N, Jenkins MW, Garrity SR, Rahn T, Powers HH, Hanson DT, Sevanto S, Wong SC, McDowell NG *et al.*, 2018. Unsaturation of vapour pressure inside leaves of two conifer species. *Scientific Reports* **8**: 7667.

Ceulemans R & Mousseau M. 1994. Effects of elevated atmospheric CO_2 on woody plants. *New Phytologist* **127**: 425-446.

Challinor AJ & Wheeler TR. 2008. Crop yield reduction in the tropics under climate change: processes and uncertainties. *Agricultural and Forest Meteorology* **148**: 343-356.

Christofferson B, Restrepo-Coupe N, Altaf Arain M, Baker IT, Cestaro BP, Ciais P, Fisher JB, Galbraith D, Guan X, Gulden L *et al.*, 2014. Mechanisms of water supply and vegetation demand govern the seasonality and magnitude of evapotranspiration in Amazonia and cerrado. *Agricultural and Forest Meteorology* **191**: 33–50.

Cochard H. 2019. A new mechanism for tree mortality due to drought and heatwaves. *bioRxiv*, 531632.

Cowan IR & Farquhar GD. 1977. Stomatal function in relation to leaf metabolism and environment. In: Integration of Activity in the Higher Plant (ed D.H. Jennings), pp. 471-505. Cambridge University Press, Cambridge.

Creese C, Oberbauer S, Rundel P, Sack L. 2014. Are fern stomatal responses to different stimuli coordinated? Testing responses to light, vapor pressure deficit, and CO_2 for diverse species grown under contrasting irradiances. *New Phytologist* **204**: 92-104.

Cunningham SC. 2004. Stomatal sensitivity to vapour pressure deficit of temperate and tropical evergreen rainforest trees of Australia. *Trees* **18**: 399-407.

Cunningham SC. 2005. Photosynthetic responses to vapour pressure deficit in temperate and tropical evergreen rainforest trees of Australia. *Oecologia* **142**: 521-528.

This article is protected by copyright. All rights reserved

Dai Z, Edwards GE, Ku MS. 1992. Control of photosynthesis and stomatal conductance in Ricinus communis L. (castor bean) by leaf to air vapor pressure deficit. *Plant Physiology* **99**: 1426-1434.

Dai AG. 2013. Increasing drought under global warming in observations and models. Nat Clim Chang. **3**: 52–58.

Dai A. 2006. Recent climatology, variability, and trends in global surface humidity, *J. Climate* **19**: 3589–3606.

Day ME. 2000. Influence of temperature and leaf-to-air vapor pressure deficit on net photosynthesis and stomatal conductance in red spruce (*Picea rubens*). *Tree Physiology* **20**: 57-63.

Dekker SC, Groenendijk M, Booth BBB, Huntingford C, Cox PM. 2016. Spatial and temporal variations in plant water-use efficiency inferred from tree-ring, eddy covariance and atmospheric observations. *Earth System Dynamics* **7**: 525-533.

Diaz-Espejo A, Buckley TN, Sperry JS, Cuevas MV, De Cires A, Elsayed-Farag S, Martin-Palomo MJ, Muriel JL, Perez-Martin A, Rodriguez-Dominguez CM, Rubio-Casal AE. 2012. Steps toward an improvement in process-based models of water use by fruit trees: a case study in olive. *Agricultural Water Management* **114**: 37-49.

Ehleringer JR, Hall AE, Farquhar GD. eds. 1993. Stable isotopes and plant carbon-water relations (Vol. 109129). San Diego: Academic Press.

Eller CB, Rowland L, Oliveira RS, Bittencourt PRL, Da Costa ACL, Meir P, Friend AD, Mencuccini M, Sitch S, Cox P. 2019. Modelling tropical forest responses to drought and El Nino with a stomatal optimisation model based on xylem hydraulics. *Philosophical Transactions of the Royal Society of London*, Series B, doi:10.1098.

Farquhar GD, Raschke K. 1978. On the resistance to transpiration of sites of evaporation within leaf. *Plant Physiology* **61**: 1000-1005.

Farquhar GD, Sharkey TD.,1982. Stomatal conductance and photosynthesis. *Annual review of plant physiology* **33**: 317-345.

Ficklin DL, Letsinger SL, Gholizadeh H, Maxwell JT. 2015. Incorporation of the Penman–Monteith potential evapotranspiration method into a Palmer Drought Severity Index tool. *Computers & Geosciences* **85**: 136-141.

This article is protected by copyright. All rights reserved

Ficklin DL & Novick KA. 2017. Historic and projected changes in vapor pressure deficit suggest a continental-scale drying of the United States atmosphere. *Journal of Geophysical Research: Atmospheres* **122**: 2061-2079.

Flexas J & Medrano H. 2002. Drought-inhibition of photosynthesis in C3 plants: stomatal and non-stomatal limitations revisited. *Annals of botany* **89**: 183-189.

Flexas J, Ribas-Carbó M, Bota J, Galmés J, Henkle M, Martínez-Cañellas S, Medrano H. 2006. Decreased Rubisco activity during water stress is not induced by decreased relative water content but related to conditions of low stomatal conductance and chloroplast CO_2 concentration. *New Phytologist* **172**: 73-82.

Flexas J., Barbour M.M., Brendel O., Cabrera H.M., Carriquí M., Diaz-Espejo A., Douthe C., Dreyer E., Ferrio J.P., Gago J, Gallé, A. 2012. Mesophyll diffusion conductance to CO2: an unappreciated central player in photosynthesis. *Plant Science* **193:** 70-84.

Francey RJ & Farquhar GD. 1982. An explanation of 13C/12C variations in tree rings. *Nature* **297**: 28.

Frank DC, Poulter B, Saurer M, Esper J, Huntingford C, Helle G, Treydte K, Zimmermann NE, Schleser GH, Ahlström A, Ciais P. 2015. Water-use efficiency and transpiration across European forests during the Anthropocene. *Nature Climate Change* **5**: 579.

Franks PJ, Cowan IR, Farquhar GD. 1997. The apparent feedforward response of stomata to air vapour pressure deficit: information revealed by different experimental procedures with two rainforest trees. *Plant, Cell & Environment* **20**: 142-145.

Franks PJ, Bonan GB, Berry JA, Lombardozzi DL, Holbrook NM, Herold N, Oleson KW. 2018. Comparing optimal and empirical stomatal conductance models for application in Earth system models. Global Change Biology **24**: 5708-5723.

Frank DC, Poulter B, Saurer M, Esper J, Huntingford C, Helle G, Treydte K, Zimmermann NE, Schleser GH, Ahlstrom A *et al.* 2015. Water-use efficiency and transpiration across European forests during the Anthropocene. *Nature Climate Change* **5**: 579-583.

Gaastra P. 1959. Photosynthesis of crop plants as influenced by light, carbon dioxide, temperature and stomatal diffusion resistance. *Mededelingen van de Landbouwhogeschool te Wageningen, Nederland* **59**: 1-68.

This article is protected by copyright. All rights reserved

Gao J, Zhao P, Shen W, Niu J, Zhu L, Ni G. 2015. Biophysical limits to responses of water flux to vapor pressure deficit in seven tree species with contrasting land use regimes. *Agricultural and forest meteorology* **200**: 258-269.

Gates DM. 1968. Transpiration and leaf temperature. *Annual Review of Plant Physiology* **19**: 211-238.

Girardin MP, Bouriaud O, Hogg EH, Kurz W, Zimmermann NE, Metsaranta JM, de Jong R, Frank DC, Esper J, Büntgen U, Guo XJ. 2016. No growth stimulation of Canada's boreal forest under half-century of combined warming and CO_2 fertilization. *Proceedings of the National Academy of Sciences* **113**: E8406-E8414.

Greve P, Roderick ML, Seneviratne SI. 2017. Simulated changes in aridity from the last glacial maximum to 4xCO2. Environmental Research Letters **12**: 114021.

Grossiord C, Sevanto S, Adams HD, Collins AD, Dickman LT, McBranch N, Michaletz ST, Stockton EA, Vigil M, McDowell NG. 2017a. Precipitation, not air temperature, drives functional responses of trees in semi-arid ecosystems. *Journal of Ecology* **105**: 163-175.

Grossiord C, Sevanto S, Borrego I, Chan AM, Collins AD, Dickman LT, Hudson PJ, McBranch N, Michaletz ST, Pockman WT, Ryan M. 2017b. Tree water dynamics in a drying and warming world. *Plant, Cell & Environment* **40**: 1861-1873.

Grossiord C, Sevanto S, Limousin JM, Meir P, Mencuccini M, Pangle RE, Pockman, WT, Salmon Y, Zweifel R, McDowell NG. 2018. Manipulative experiments demonstrate how long-term soil moisture changes alter controls of plant water use. *Environmental and Experimental Botany* **152**: 19-27.

Hanson PJ, Childs KW, Wullschleger SD, Riggs JS, Thomas WK, Todd DE, Warren JM. 2011. A method for experimental heating of intact soil profiles for application to climate change experiments. *Global Change Biology* **17**: 1083–1096.

Hall AE, Kaufmann MR. 1975. Stomatal Response to Environment with *Sesamum indicum*. L. *Plant Physiology* **55**: 455-459.

Harris I, Jones PD, Osborn TJ, Lister DH. 2013. Updated high-resolution grids of monthly climatic observations – the CRU TS3.10 Dataset. *International Journal of Climatology* **34**: 623–642.

This article is protected by copyright. All rights reserved

Harris IPDJ, Jones PD, Osborn TJ, Lister DH. 2014. Updated high-resolution grids of monthly climatic observations–the CRU TS3. 10 Dataset. *International journal of climatology* **34**: 623-642.

Hatfield JL, Prueger JH. 2015. Temperature extremes: Effect on plant growth and development. *Weather and climate extremes*, **10**: 4-10.

Hickler T, Prentice IC, Smith B, Sykes MT, Zaehle S. 2006. Implementing plant hydraulic architecture within the LPJ dynamic global vegetation model. *Global Ecology and Biogeography* **15**: 567–577.

Holloway-Phillips M-M, Cernusak LA, Stuart-Williams H, Ubierna N, Farquhar GD. 2019. Two-source $\delta^{18}O$ method to validate the $CO^{18}O$-photosynthetic discrimination model: implications for g_m. *Plant Physiology* **181**: 1175-1190.

Hölscher D, Koch O, Korn S, Leuschner C. 2005. Sap flux of five co-occurring tree species in a temperate broad-leaved forest during seasonal soil drought. *Trees* **19**: 628-637.

Hölttä T, Lintunen A, Chan T, Mäkelä A, Nikinmaa E. 2017. A steady-state stomatal model of balanced leaf gas exchange, hydraulics and maximal source–sink flux. *Tree Physiology* **37**: 851-868.

Howell TA & Dusek DA. 1995. Comparison of vapor-pressure-deficit calculation methods—southern high plains. *Journal of irrigation and drainage engineering* **121**: 191-198.

Huang CW, Domec JC, Palmroth S, Pockman WT, Litvak ME, Katul GG. 2018. Transport in a coordinated soil-root-xylem-phloem leaf system. *Advances in Water Resources* **119**: 1-16.

Hughes L. 2000. Biological consequences of global warming: is the signal already apparent?. *Trends in Ecology & Evolution* **15**: 56-61.

Hulley G, Hook S, Fisher J, Lee C. 2017. July. ECOSTRESS, A NASA Earth-Ventures Instrument for studying links between the water cycle and plant health over the diurnal cycle. In *Geoscience and Remote Sensing Symposium (IGARSS), 2017 IEEE International* (pp. 5494-5496). IEEE.

Huntington TG. 2006. Evidence for intensification of the global water cycle: review and synthesis. *Journal of Hydrology* **319**: 83-95.

This article is protected by copyright. All rights reserved

Humphrey V, Zscheischler J, Ciais P, Gudmundsson L, Sitch S, Seneviratne SI. 2018. Sensitivity of atmospheric CO_2 growth rate to observed changes in terrestrial water storage. *Nature* **560**: 628–631.

Intergovernmental Panel on Climate Change. 2019. Climate Change and Land: An IPCC Special Report on climate change, desertification, land degradation, sustainable land management, food security, and greenhouse gas fluxes in terrestrial (Summary for Policymakers) ecosystems. Intergovernmental Panel on Climate Change (IPCC): Geneva.

Ishibashi M, Terashima I. 1995. Effects of continuous leaf wetness on photosynthesis: adverse aspects of rainfall. *Plant, Cell & Environment* **18**: 431–438

Jarvis PG, Slatyer RO. 1970. The role of the mesophyll cell wall in leaf transpiration. *Planta* **90**: 303-322.

Jarvis PG. 1976. The interpretation of the variations in leaf water potential and stomatal conductance found in canopies in the field. *Philosophical Transactions of the Royal Society London*, Series B, **273**: 593-610.

Jones HG, Higgs KH. 1980. Resistance to water loss from mesophyll cell surface in plant leaves. *Journal of Experimental Botany* **31**: 545-553.

Jung M, Reichstein M, Schwalm CR, Huntingford C, Sitch S, Ahlstrom A, Arneth A, Camps-Valls G, Ciais P, Friedlingstein P *et al*., 2017. Compensatory water effects link yearly global land CO_2 sink changes to temperature. *Nature* **541**: 516.

Katul G, Manzoni S, Palmroth S, Oren R. 2009. A stomatal optimization theory to describe the effects of atmospheric CO_2 on leaf photosynthesis and transpiration. *Annals of Botany* **105**: 431-442.

Keel S, Pepin S, Leuzinger S, Körner C. 2007. Stomatal conductance in mature deciduous forest trees exposed to elevated CO_2. *Trees* **21**: 151-159.

Kennedy D, Swenson SC, Oleson KW, Lawrence DM, Fisher RA, Lola da Costa AC, Gentine P. 2019. Implementing plant hydraulics in the community land model, version 5. Journal of Advances in Modeling Earth Systems. *Journal of Advances in Modeling Earth Systems* **11**: 485-513

This article is protected by copyright. All rights reserved

Kim J, Verma SB. 1991. Modeling canopy stomatal conductance in a temperate grassland ecosystem. *Agricultural and forest meteorology* **55**: 149-166.

Klein T. 2014. The variability of stomatal sensitivity to leaf water potential across tree species indicates a continuum between isohydric and anisohydric behaviours. *Functional Ecology* **28**: 1313-1320.

Knapp AK, Avolio ML, Beier C, Carroll CJ, Collins SL, Dukes JS, Fraser LH, Griffin-Nolan RJ, Hoover DL, Jentsch A, Loik ME. 2017. Pushing precipitation to the extremes in distributed experiments: recommendations for simulating wet and dry years. *Global change biology* **23**: 1774-1782.

Körner C, Neumayer M, Menendezriedl SP, Smeets-scheel A. 1989. Functional morphology of mountain plants. *Flora* **182**: 353-383

Krinner G, Viovy N, de Noblet-Ducoudré N, Ogeé J, Polcher J, Friedlingstein P, Ciais P, Sitch S, Prentice IC. 2005. A dynamic global vegetation model for studies of the coupled atmosphere-biosphere system. *Global Biogeochemical Cycles* **19**, GB1015, doi:10.1029/2003GB002199.

Kupper P, Sõber J, Sellin A, Lõhmus K, Tullus A, Räim O, Lubenets K, Tulva I, Uri V, Zobel M, Kull O. 2011. An experimental facility for free air humidity manipulation (FAHM) can alter water flux through deciduous tree canopy. *Environmental and Experimental Botany* 72: 432-8.

Kwon H, Law BE, Thomas CK, Johnson BG. 2018. The influence of hydrological variability on inherent water use efficiency in forests of contrasting composition, age, and precipitation regimes in the Pacific Northwest. *Agricultural and Forest Meteorology* **249**: 488-500.

Leuning R. 1995. A critical appraisal of a coupled stomatal-photosynthesis model for C3 plants. *Plant Cell & Environment* **18**: 339-357.

Li X, Gentine P, Lin C, Zhou S, Sun Z, Zheng Y, Liu J, Zheng, C. 2019. A simple and objective method to partition evapotranspiration into transpiration and evaporation at eddy-covariance sites. *Agricultural and Forest Meteorology* **265**:171-182.

This article is protected by copyright. All rights reserved

Lindner M, Maroschek M, Netherer S, Kremer A, Barbati A, Garcia-Gonzalo J, Seidl R, Delzon S, Corona P, Kolstrom M *et al*. 2010. Climate change impacts, adaptive capacity, and vulnerability of European forest ecosystems. *Forest Ecology and Management* **259**: 698-709.

Lloyd J. 1991. Modeling stomatal responses to environment in Macadamia integrifolia. *Australian Journal of Plant Physiology* **18**: 649-660.

Lobell DB, Schlenker W, Costa-Roberts J. 2011. Climate trends and global crop production since 1980. *Science* **333**:616-20.

Lobell DB, Hammer GL, McLean G, Messina C, Roberts MJ, Schlenker W. 2013. The critical role of extreme heat for maize production in the United States. *Nature Climate Change* **3**: 497.

Lohammer T, Larsson S, Linder S, Falk SO. 1980. FAST-Simulation models of gaeous exchange in Scots Pine. *Ecological Bulletin* **32**: 505-523.

Long SP, Woolhouse HW. 1978. The responses of net photosynthesis to vapor pressure deficit and CO2 concentration in Spartina townsendii (sensu lato), a C4 species from a cool temperate climate. *Journal of Experimental Botany* **29**:567-577

Mahan JR, Upchurch DR. 1988. Maintenance of constant leaf temperature by plants—I. Hypothesis-limited homeothermy. *Environmental and Experimental Botany* **28**: 351-357.

Marchin RM, Broadhead AA, Bostic LE, Dunn RR, Hoffmann WA. 2016. Stomatal acclimation to vapour pressure deficit doubles transpiration of small tree seedlings with warming. *Plant, Cell & Environment* **39**: 2221-2234.

Martinez-Vilalta J, Poyatos R, Aguade D, Retana J, Mencuccini M. 2014. A new look at water transport regulation in plants. New Phytologist **204**: 105-115.

McAdam SA, Brodribb TJ. 2016. Linking turgor with ABA biosynthesis: implications for stomatal responses to vapor pressure deficit across land plants. *Plant Physiology* **171**: 2008-2016.

McCarthy MP, Thorne PW, Titchner HA. 2009. An analysis of tropospheric humidity trends from radiosondes. *J. Climate* **22**: 5820–5838.

This article is protected by copyright. All rights reserved

McDowell NG, Beerling DJ, Breshears DD, Fisher RA, Raffa KF, Stitt M. 2011. The interdependence of mechanisms underlying climate-driven vegetation mortality. *Trends in Ecology and Evolution* **26**: 523–532.

McDowell NG, Williams AP, Xu C, Pockman WT, Dickman LT, Sevanto S, Pangle R, Limousin J, Plaut J, Mackay DS *et al.* 2016. Multi-scale predictions of massive conifer mortality due to chronic temperature rise. *Nature Climate Change* **6** :295.

McDowell NG, Allen CD, Anderson-Teixeira K, Brando P, Brienen R, Chambers J, Christoffersen B, Davies S, Doughty C, Duque A *et al.* 2018. Drivers and mechanisms of tree mortality in moist tropical forests. *New Phytologist* **219**: 851-869.

McNaughton KG, Jarvis PG. 1991. Effects of spatial scale on stomatal control of transpiration. *Agricultural and Forest Meteorology* **54**: 279–301.

Medlyn BE, Duursma RA, Eamus D, Ellsworth DS, Prentice IC, Barton CVM, Crous KY, De Angelis P, Freeman M, Wingate L. 2011. Reconciling the optimal and empirical approaches to modelling stomatal conductance. *Global Change Biology* **17**: 2134-2144.

Mencuccini M, Manzoni S, Christoffersen B. 2019. Modelling water fluxes in plants: from tissues to biosphere. *New Phytologist*, https://doi.org/10.1111/nph.15681.

Meinzer FC. 2003. Functional convergence in plant responses to the environment. *Oecologia* **134**: 1-11.

Moorcroft PR, Hurtt GC, Pacala SW. 2001. A method for scaling vegetation dynamics: The ecosystem demography model (ED). *Ecological Monographs* **71**: 557–586.

Monteith JL. 1965. Evaporation and environment. In: Fogg BD (ed). The State and Movement of water 625 in Living Organisms, Symposium of the Society of Experimental Biology, **19**: 205-234, Cambridge University Press, UK

Monteith JL, Unsworth MH. 1990. Principles of environmentul Physics, 2nd edition, Edward Arnold, London, 291 pp.

Monteith JL. 1995. A reinterpretation of stomatal responses to humidity. *Plant, Cell & Environment* **18**: 357-364.

Mott KA, Parkhurst DF. 1991. Stomatal responses to humidity in air and helox. *Plant, Cell & Environment* **14**: 509-515.

This article is protected by copyright. All rights reserved

Mott KA, Peak D. 2010. Stomatal responses to humidity and temperature in darkness. *Plant, Cell & Environment* **33**: 1084-1090.

Nicotra AB, Atkin OK, Bonser SP, Davidson AM, Finnegan EJ, Mathesius U, Poot P, Purugganan MD, Richards CL, Valladares F *et al*. 2010) Plant phenotypic plasticity in a changing climate. *Trends in Plant Science* **15**: 684-692.

Novick KA, Ficklin DL, Stoy PC, Williams CA, Bohrer G, Oishi AC, Papuga SA, Blanken PD, Noormets A, Sulman BN, Scott RL. 2016. The increasing importance of atmospheric demand for ecosystem water and carbon fluxes. *Nature Climate Change* **6**: 1023.

Novick KA, Konings AG, Gentine P. 2019. Beyond soil water potential: An expanded view on isohydricity including land–atmosphere interactions and phenology. *Plant, Cell & Environment*, 10.1111/pce.13517

O'Gorman PA, Muller CJ. 2010. How closely do changes in surface and column water vapor follow Clausius–Clapeyron scaling in climate change simulations?. *Environmental Research Letters*, **5**: 025207.

Oksanen E, Lihavainen J, Keinänen M, Keski-Saari S, Kontunen-Soppela S, Sellin A, Sõber A. 2018. Northern forest trees under increasing atmospheric humidity. *Progress in Botany* **80**: 317-336.

Oren R, Sperry JS, Katul GG, Pataki DE, Ewers BE, Phillips N, Schäfer KVR. 1999. Survey and synthesis of intra-and interspecific variation in stomatal sensitivity to vapour pressure deficit. *Plant, Cell & Environment* **22**: 1515-1526.

Pataki DE, Oren R, Phillips N. 1998a. Responses of sap flux and stomatal conductance of *Pinus taeda* L. trees to stepwise reductions in leaf area. *Journal of Experimental Botany* **49:** 871-878.

Pataki DE, Oren R, Katul G, Sigmon J. 1998b. Canopy conductance of Pinus taeda, Liquidambar styraciflua and Quercus phellos under varying atmospheric and soil water conditions. *Tree Physiology* **18**: 307-315.

Penman HL. 1948. Natural Evaporation from Open Water, Bare Soil and Grass. Proceedings of the 622 Royal Society of London Series a-Mathematical and Physical Sciences **193**: 120.

Pieruschka RGH, Berry JA. 2010. Control of transpiration by radiation. *Proceedings of the National Academy of Sciences of the United States of America* **107**: 13372-13377.

This article is protected by copyright. All rights reserved

Accepted Article

Prentice IC, Bondeau A, Cramer W, Harrison SP, Hickler T, Lucht W, Sitch S, Smith B, Sykes MT. 2007. Dynamic global vegetation modeling: Quantifying terrestrial ecosystem responses to large-scale environmental change. Pages 175–192 in P. Canadell, D. E. Pataki, and L. F. Pitelka, editors. Terrestrial Ecosystems in a Changing World. Springer-Verlag, Berlin, Heidelberg, DE.

Raczka B, Davis KJ, Huntzinger D, Neilson RP, Poulter B, Richardson A, Xiao J, Baker I, Ciais P, Keenan TF, Law B, Post W, Ricciuto D, Schaefer K, Tian H, Tomelleri E, Verbeeck H, Viovy N. 2013. Evaluation of continental carbon cycle simulations with North American flux tower observations. *Ecological Monographs* **83**: 531–556.

Rashid MA, Andersen MN, Wollenweber B, Zhang X, Olesen JE. 2018. Acclimation to higher VPD and temperature minimized negative effects on assimilation and grain yield of wheat. *Agricultural and forest meteorology* **248**: 119-129.

Restaino CM, Peterson DL, Littell J. 2016. Increased water deficit decreases Douglas fir growth throughout western US forests. *Proceedings of the National Academy of Sciences* **113**: 9557-9562.

Rigden AJ, Salvucci GD, Entekhabi D, Short Gianotti DJ. 2018. Partitioning evapotranspiration over the continental United States using weather station data. *Geophysical Research Letters* **45**: 9605-9613.

Roderick M, Sun F, Lim WH, Farquhar G. 2014. A general framework for understanding the response of the water cycle to global warming over land and ocean. *Hydrology and Earth System Sciences* **18**: 1575-1589.

Rodriguez-Dominguez CM, Buckley TN, Egea G, de Cires A, Hernandez-Santana V, Martorell S, Diaz-Espejo A. 2016. Most stomatal closure in woody species under moderate drought can be explained by stomatal responses to leaf turgor. *Plant, Cell & Environment* **39**: 2014-2026.

Rowland L, Harper A, Christoffersen BO, Galbraith D, Imbuzeiro HMA, Powell TL, Doughty C, Levine NM, Malhi H, Saleska SR, Moorcroft PR, Meir P, Williams M. 2015. Modelling climate change responses in tropical forests: similar productivity estimates across five models, but different mechanisms and responses. *Geoscientific Model Development* 8: 1097-1110.

This article is protected by copyright. All rights reserved

Running SW. 1976. Environmental control of leaf water conductance in conifers. *Can. J. For. Res*. **6**: 104–112.

Sadler EJ, Evans DE. 1989. Vapor pressure deficit calculations and their effect on the comhination equation. *Agric. and For. Meterology* **49**: 55-80.

Schoppach R, Sadok W. 2013. Transpiration sensitivities to evaporative demand and leaf areas vary with night and day warming regimes among wheat genotypes. *Functional Plant Biology* **40**: 708-718.

Schymanski SJ, Or D. 2017. Leaf-scale experiments reveal an important omission in the Penman-Monteith equation. *Hydrology & Earth System Sciences* **21**: 685-706.

Seager R, Hooks A, Williams AP, Cook B, Nakamura J, Henderson N. 2015. Climatology, variability, and trends in the U.S. Vapor pressure deficit, an important fire-related meteorological quantity. *J. Appl. Meteorol. Climatol*. **54**: 1121–1141.

Sellers P, Randall DA, Collatz GJ, Berry JA, Field CB, Dazlich D, Zhang C, Collelo GD, Bounoua L. 1996. A revised land surface parameterization (SiB2) for atmospheric GCMs. Part I: Model formulation. *Journal of Climate* **9**: 676–705.

Sharpe PJ, Wu HI, Spence RD. 1987. Stomatal mechanics. *Stomatal function* 91-114.

Shenbin C, Yunfeng L, Thomas A. 2006. Climatic change on the Tibetan Plateau: Potential evapotranspiration trends from 1961– 2000. *Climatic Change* **76**: 291–319.

Sherwood SC, Ingram W, Tsushima Y, Satoh M, Roberts M, Vidale PL, O'Gorman PA. 2010. Relative humidity changes in a warmer climate. *Journal of Geophysical Research: Atmospheres* **115**, doi: 10.1029/2009JD012585.

Sitch S, Friedlingstein P, Gruber N, Jones SD, Murray-Tortarolo G, Ahlström A, Doney SC, Graven H, Heinze C, Huntingford C *et al.* 2013. Recent trends and drivers of regional sources and sinks of carbon dioxide. *Biogeosciences* **12**, 653–679.

Sitch S, Smith B, Prentice IC, Arneth A, Bondeau A, Cramer W, Kaplan JO, Levis S, Lucht W, Sykes MT, Thonicke K, Venevsky S. 2003. Evaluation of ecosystem dynamics, plant geography and terrestrial carbon cycling in the LPJ dynamic global vegetation model. *Global Change Biology* **9**,161–185.

This article is protected by copyright. All rights reserved

Sperry JS, Venturas MD, Anderegg WR, Mencuccini M, Mackay DS, Wang Y, Love DM. 2017. Predicting stomatal responses to the environment from the optimization of photosynthetic gain and hydraulic cost. *Plant, Cell & Environment* **40**: 816-830.

Stocker BD, Zscheischler J, Keenan TF, Prentice IC, Seneviratne SI, Peñuelas J. 2019. Drought impacts on terrestrial primary production underestimated by satellite monitoring. *Nature Geoscience* **12**: 264–270.

Stovall AE, Shugart H, Yang X. 2019. Tree height explains mortality risk during an intense drought. *Nature communications* **10**: 1-6.

Streck NA. 2003. Stomatal response to water vapor pressure deficit: an unsolved issue. *Current Agricultural Science and Technology* **9**.

Sulman BN, Roman DT, Yi K, Wang L, Phillips RP, Novick KA. 2016. High atmospheric demand for water can limit forest carbon uptake and transpiration as severely as dry soil. *Geophysical Research Letters* **43**: 9686-9695.

Teskey R, Wertin T, Bauweraerts I, Ameye M, McGuire MA, Steppe K. 2015. Responses of tree species to heat waves and extreme heat events. *Plant, cell & environment* 38: 1699-712.

Tyree MT, Sperry JS. 1988. Do woody plants operate near the point of catastrophic xylem dysfunction caused by dynamic water stress? Answers from a model. *Plant Physiology* **88**: 574-580.

Urban J, Ingwers M, McGuire MA, Teskey RO. 2017. Stomatal conductance increases with rising temperature. *Plant signaling & behavior* **12**: e1356534.

Valladares F, Pearcy RW. 2002. Drought can be more critical in the shade than in the sun: a field study of carbon gain and photo-inhibition in a Californian shrub during a dry El Ni~no year. *Plant, Cell and Environment* **25**: 749–759.

Venturas MD, Sperry JS, Love DM, Frehner EH, Allred MG, Wang Y, Anderegg WR. 2018. A stomatal control model based on optimization of carbon gain versus hydraulic risk predicts aspen sapling responses to drought. *New Phytologist* **220**: 836-850.

Wahid A, Gelani S, Ashraf M, Foolad MR. 2007. Heat tolerance in plants: An overview. *Environmental and Experimental Botany* **61**: 199-223.

Accepted Article

This article is protected by copyright. All rights reserved

Walker AP, Beckerman AP, Gu LH, Kattge J, Cernusak LA, Domingues TF, Scales JC, Wohlfahrt G, Wullschleger SD, Woodward FI. 2014. The relationship of leaf photosynthetic traits - V_{cmax} and J_{max} - to leaf nitrogen, leaf phosphorus, and specific leaf area: a meta-analysis and modeling study. *Ecology and Evolution* **4**: 3218-3235.

Wang H, Guan H, Simmons CT. 2016. Modeling the environmental controls on tree water use at different temporal scales. *Agricultural and forest meteorology* **225**: 24-35.

Wang M, Chen Y, Wu X, Bai Y. 2018. Forest-Type-Dependent Water Use Efficiency Trends Across the Northern Hemisphere. *Geophysical Research Letters* **45**: 8283-8293.

Ward DA, Bunce JA. 1986. Novel evidence for a lack of water-vapor saturation within the intercellular airspace of turgid leaves of mesophytic species. *Journal of Experimental Botany* **37**: 504-516.

Way DA, Oren R. 2010. Differential responses to changes in growth temperature between trees from different functional groups and biomes: a review and synthesis of data. *Tree Physiology* **30**: 669-688.

Whitehead D, Okali DUU, Fasehun FE. 1981. Stomatal response to environmental variables in two tropical forest species during the dry season in Nigeria. *Journal of Applied Ecology* **18**: 571–587.

Will RE, Wilson SM, Zou CB, Hennessey TC. 2013. Increased vapor pressure deficit due to higher temperature leads to greater transpiration and faster mortality during drought for tree seedlings common to the forest–grassland ecotone. *New Phytologist* 200: 366-74.

Willett KM, Gillett NP, Jones PD, Thorne PW. 2007. Attribution of observed surface humidity changes to human influence. *Nature* **449**: 710.

Williams M, Rastetter EB, Fernandes DN, Goulden ML, Wofsy SC, Shaver GR, Melillo JM, Munger JW, Fan SM, Nadelhoffer KJ. 1996. Modelling the soil-atmosphere continuum in a Quercus-Acer stand at Harvard Forest: The regulation of stomatal conductance by light, nitrogen and soil/plant hydraulic properties. *Plant Cell & Environment* **19**: 911-927.

Williams AP, Allen CD, Macalady AK, Griffin D, Woodhouse CA, Meko DM, Swetnam TW, Rauscher SA, Seager R, Grissino-Mayer HD *et al*. 2013. Temperature as a potent driver of regional forest drought stress and tree mortality. *Nat. Clim. Change* **3**: 292–297.

This article is protected by copyright. All rights reserved

Williams AP, Seager R, Berkelhammer M, Macalady AK, Crimmins MA, Swetnam TW, Trugman AT, Buenning N, Hryniw N, McDowell NG *et al*. 2014. Causes and implications of extreme atmospheric moisture demand during the record-breaking 2011 wildfire season in the southwestern United States, *J. Appl. Meteorol. Climatol*. **53**: 2671–2684.

Wullschleger SD. 1993. Biochemical limitations to carbon assimilation in C_3 plants - a retrospective analysis of the A/C_i curves from 109 species. *Journal of Experimental Botany* **44**: 907-920.

Yong JWH, Wong SC, Farquhar GD. 1997. Stomatal response to changes in vapour pressure difference between leaf and air. *Plant, Cell & Environment* **20**: 1213-1216.

Yuan W, Zheng Y, Piao S, Ciais P, Lombardozzi D, Wang Y, Ryu Y, Chen G, Dong W, Hu Z, Jain AK. 2019. Increased atmospheric vapor pressure deficit reduces global vegetation growth. *Science advances* **5**: eaax1396.

Zhao J, Hartmann H, Trumbore S, Ziegler W, Zhang Y. 2013. High temperature causes negative whole-plant carbon balance under mild drought. *New phytologist* 200: 330-9.

Zhao C, Liu B, Piao S, Wang X, Lobell DB, Huang Y, Huang M, Yao Y, Bassu S, Ciais P, Durand JL. 2017. Temperature increase reduces global yields of major crops in four independent estimates. *Proceedings of the National Academy of Sciences* **114**:9326-31.

Zhang K, Kimball JS, Nemani RR, Running SW, Hong Y, Gourley JJ, Yu Z. 2015. Vegetation greening and climate change promote multidecadal rises of global land evapotranspiration. *Sci. Rep.* **5**, doi:10.1038/srep15956.

Zhang Q, Ficklin D, Manzoni S., Wang L, Way D., Phillips RP, Novick KA. 2019. Response of ecosystem intrinsic water use efficiency and gross primary productivity to rising vapor pressure deficit. Environmental Research Letters **14**, doi: 10.1088/1748-9326/ab2603.

This article is protected by copyright. All rights reserved

Accepted Article

Supporting information:

Figure S1. Response of net CO_2 assimilation rate to leaf-to-air vapor pressure deficit in four species.

This article is protected by copyright. All rights reserved

Box 1 List of abbreviations

VPD = air vapor pressure deficit (commonly in kPa)

VPD_L = leaf-to-air vapor pressure deficit (commonly in kPa)

e_s = saturation vapor pressure (commonly in kPa)

e_a = actual vapor pressure (commonly in kPa)

RH = relative humidity in the atmosphere (commonly in %)

g_s = stomatal conductance (commonly in mol of H_2O m^{-2} s^{-1})

g_{sref} = g_s at 1 kPa VPD

Ψ_L = leaf water potential (commonly in MPa)

K_{leaf} = leaf hydraulic conductance (commonly in mmol of H_2O m^{-2} s^{-1} MPa^{-1})

G_{surf} = stand-level surface canopy conductance (commonly in mol of H_2O m^{-2} s^{-1})

A = photosynthetic CO_2 assimilation (commonly in μmol of CO_2 m^{-2} s^{-1})

T = transpiration (commonly in mm of H_2O d^{-1})

$\delta^{13}C$ = carbon isotopic composition (commonly in ‰)

c_i/c_a = the ratio of intercellular (c_i) to ambient (c_a) CO_2 concentrations

$[CO_2]$ = atmospheric carbon dioxide concentration (commonly in ppm)

m = slope between g_s and ln(VPD) (commonly in mol of H_2O m^{-2} s^{-1}ln(Kpa))

ET = evapotranspiration (commonly in mm of H_2O d^{-1})

NPP= net primary productivity (commonly in g C m^{-2} y^{-1})

GEP = gross ecosystem-level productivity (commonly in g C m^{-2} y^{-1})

$iWUE$ = intrinsic water use efficiency (commonly in μmol of CO_2 mol^{-1} of H_2O)

λ = Lagrange multiplier

P = leaf xylem pressure (commonly in MPa)

K = soil-to-canopy hydraulic conductance per leaf area (commonly in mmol of H_2O m^{-2} s^{-1} MPa^{-1})

P_{soil} = soil water potential (commonly in MPa)

V_{cmax} = maximum carboxylation velocity (commonly in μmol of CO_2 m^{-2} s^{-1})

J_{max} = maximum rate of electron transport (commonly in μmol of CO_2 m^{-2} s^{-1})

This article is protected by copyright. All rights reserved

Figure legends

Figure 1: Trend in annual vapor pressure deficit (*VPD*) for the period 1901-2017 estimated using *VPD* calculated from air temperature and vapor pressure from the Climate Research Unit (CRU) version TS 3.26 (Harris *et al*., 2014) with regional boundaries superimposed (a), and percent change in *VPD* relative to 1901 averaged for regions. Bold lines have a 10-year smoothing function applied (BNA, Boreal North America; TNA, Temperate North America; TRSA, Tropical South America; TESA, Temperate South America; NAf, Northern Africa; SAf, Southern Africa; BEu, Boreal Eurasia; TEu, Temperate Eurasia; TAs, Tropical Asia; AUS, Australia; EUR, Europe; NAfs, Northern Africa semi-arid; SAfs, Southern Africa semi-arid) (b).

Figure 2: Relationship between atmospheric vapor pressure (kPa), and relative humidity (%) as a function of air temperature. The bold line represents the saturation vapor pressure (e_s) as a function of temperature (i.e. 100% humidity at any given temperature). Vapor pressure deficit (*VPD*, kPa) represents the difference between e_s (i.e. bold line) and the actual vapor pressure at a given temperature (dotted lines). Panel (a) shows shifts in *VPD* for one scenario representing typical temperature changes during extreme heat waves: relative humidity remains constant at 20% (red dotted line) but temperature increase from 25°C to 35°C resulting in an increase in *VPD* of 2.0 kPa (i.e. from 2.5 kPa to 4.5 kPa, red arrows). Panel (b) shows shifts in *VPD* corresponding to projected long-term changes in temperature and humidity under a business-as-usual scenario: relative humidity remains stable (20%; red dotted line) and air temperature rises by 5°C (from 25°C to 30°C) resulting in an increase in *VPD* of 0.9 kPa (i.e. from 2.5 kPa to 3.4 kPa, red and yellow arrow). The figure highlights that with rising temperature we should expect a simultaneous increase in *VPD* both under extreme events (a) as well as on the long-term (b).

Figure 3: Sample steady state (a) and dynamic (b) responses of stomatal conductance (g_s) to *VPD*. Data are reproduced from (a) Mott & Parkhurst (1991), and (b) Buckley (2016). In (a), the symbols are experimental measurements, and the lines are theoretical responses using the empirical model of Oren *et al*. (1999) ($g_s = g_{s,ref} \cdot (1 - m \cdot \ln(VPD/VPD_{ref}))$, where g_{sref} is the value of g_s at $VPD = VPD_{ref} = 1$ kPa (taken from the experimental measurements in this example; $g_{s,ref} = 0.43$ mol m^{-2} s^{-1}), and m represents the slope between g_s and $\ln(VPD)$; the numbers shown to the right of each line is the corresponding value of m.

Figure 4: Eddy covariance flux data are useful for understanding how the response of surface conductance (left column) and gross ecosystem productivity (right column) respond to vapor

This article is protected by copyright. All rights reserved

pressure deficit (*VPD*). When shown as absolute vales, both conductance and gross ecosystem productivity (*GEP*) are negatively related to *VPD*, but the variability from one site to the next is quite large (see absolute values). However, if the site-level data are normalized by their rates at a reference *VPD* of 1 kPa, the cross-site variability at a given *VPD* is considerably reduced, particularly for conductance (see relative values). As predicted from theory, the sensitivity of conductance to *VPD* (*m*) is greater than the sensitivity of *GEP* to changes in *VPD*, reflecting that fact that intrinsic water use efficiency (iWUE) often increases with rising *VPD*. The gray shaded area shows the range of the model $y = 1 - m \cdot \ln(VPD)$, for the range of *m* represent +/- 3 S.E. for the slope parameter derived from linear regression. Data represent a subset of the FLUXNET Tier1 tower sites, where *GEP* is provided by FLUXNET, and G_s is estimated following the approach of Novick *et al*. (2016). To reduce confounding effects from radiation and soil moisture, which co-vary with *VPD*, this analysis was limited to periods of high radiation (> 400 W/m^2) and the site-specific curves represent the average of responses determined within unique soil moisture bins ($n = 5$ at each site).

Figure 5: Conceptual figure highlighting the potential mechanisms of hydraulic failure and carbon starvation during drought under low and high vapor pressure deficit (*VPD*). After drought inception (red dashed vertical line) and under constant low (blue) or high (orange) *VPD*, evapotranspiration (*ET*) will decrease as soil moisture declines but the drop in *ET* will occur earlier and be faster under high *VPD*. Thus, hydraulic failure (defined here as the percentage loss of conductance, *PLC,* the orange dashed and dotted blue lines) will occur faster under high *VPD* due to increasing embolism (a); growth (dotted black line) and carbon uptake through photosynthesis will decline more rapidly under higher *VPD* due to lower *PLC* and increasing tissue temperature (b); non-structural carbohydrates (NSC) content and defensive capacity increases for a short term due to the imbalance of growth and photosynthesis declines, with a more rapid NSC and defensive capacity loss in higher *VPD* environments (c). Ultimately, the risk of drought-induced mortality through hydraulic failure (a) and carbon starvation (c) are higher and more rapid under increasing *VPD*.

This article is protected by copyright. All rights reserved

Figure 6: Nine model scenarios of the stomatal response to leaf-to-atmosphere vapor pressure deficit, VPD_L. (a) Response of leaf diffusive conductance to water vapor (G_L). (b) Response of leaf transpiration rate (T). Red curve is the gain-risk model and the dashed blue is the $\lambda = dT/dA$ model, where λ is constant at the initial (low VPD_L) value from the gain-risk simulation (curves from Sperry *et al*., 2017). The seven remaining curves were fit to maximize the r^2 with the red gain-risk G_L to facilitate comparison. Five of these curves have G_L proportional to $f(VPD_L) \bullet A$, where A is the photosynthetic rate taken from the red gain-risk curve. Their five f(VPD) functions were as follows: pink, $1/(1+ VPD_L /VPD_o)$(Lohammer *et al.,* 1980); grey, $1/ VPD_L$ (Lloyd, 1991); cyan, $1/ VPD_L^{0.5}$ (Lloyd 1991); brown, $1- VPD_L/ VPD_o$ (Jarvis ,1976); green, RH, where VPD_L was converted to relative humidity (RH) (Ball *et al.,* 1987). The last two curves have G_L proportional to $f(VPD_L)$. The $f(VPD_L)$ functions were: black, $g_{sref} - m \ln (VPD_L)$ ($g_{sref} = G_L$ at $VPD_L = 1$ kPa); yellow: $1/ VPD_L$ (Oren *et al.,* 1999). VPD_o, g_{sref}, and m are curve fitting parameters.

This article is protected by copyright. All rights reserved

Accepted Article

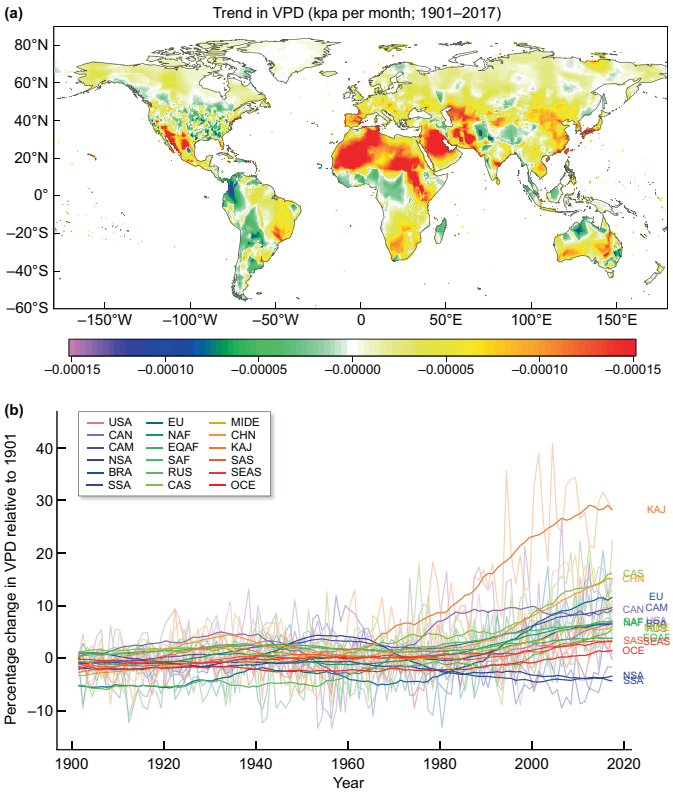

Figure 1

Tansley Review 30269

This article is protected by copyright. All rights reserved

Accepted Article

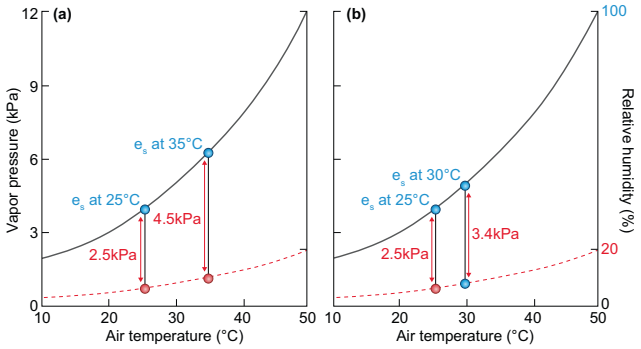

Figure 2

Tansley Review 30269

This article is protected by copyright. All rights reserved

Accepted Article

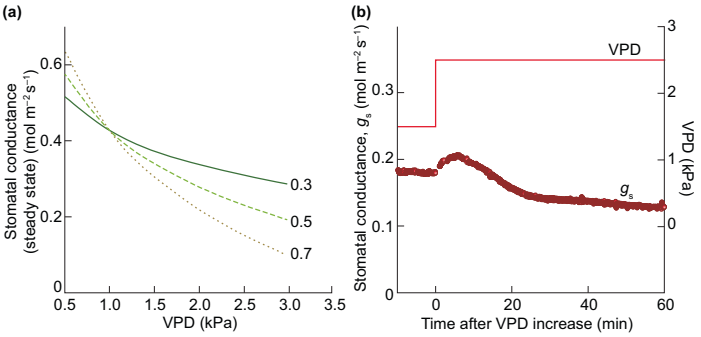

Figure 3

Tansley Review 30269

This article is protected by copyright. All rights reserved

Accepted Article

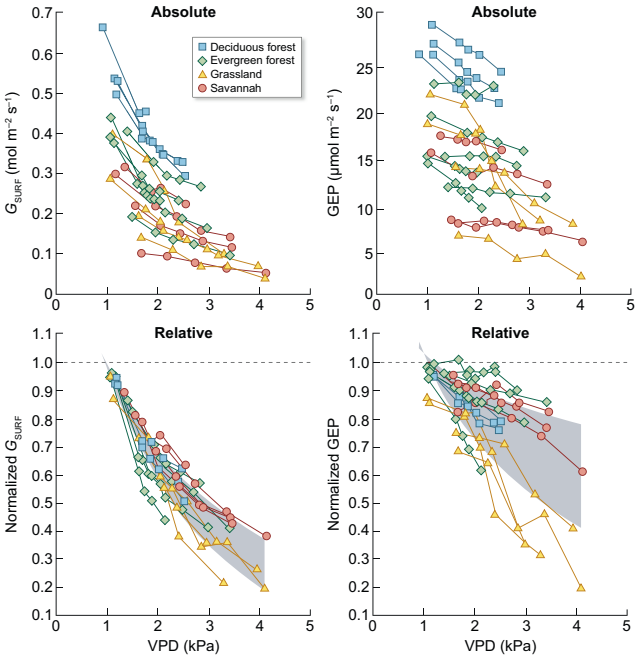

Figure 4

Tansley Review 30269

This article is protected by copyright. All rights reserved

Accepted Article

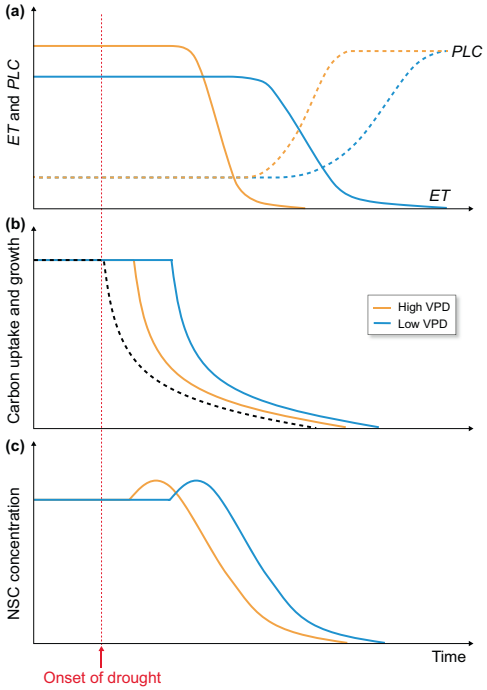

Figure 5

Tansley Review 30269

This article is protected by copyright. All rights reserved

Accepted Article

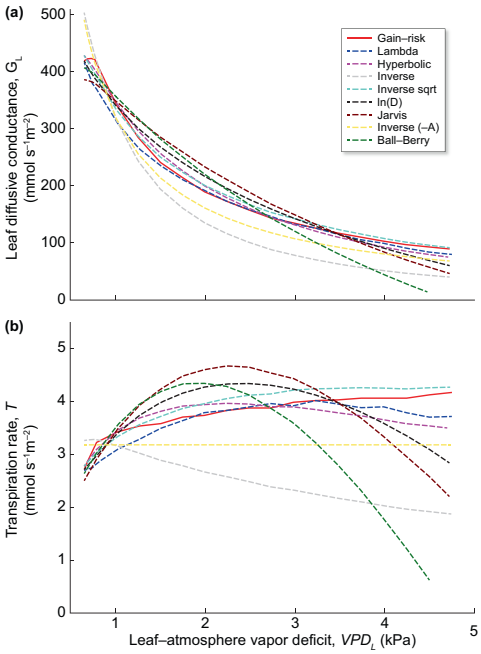

Figure 6

Tansley Review 30269

This article is protected by copyright. All rights reserved